Title

A role for the Smc3 hinge domain in the maintenance of sister chromatid cohesion

Journal

Molecular Biology of the Cell, 29(3)

ISSN

1059-1524

Authors

Robison, Brett
Guacci, Vincent
Koshland, Douglas

Publication Date

2018-02-01

DOI

10.1091/mbc.e17-08-0511

Peer reviewed

A role for the Smc3 hinge domain in the maintenance of sister chromatid cohesion

Brett Robison, Vincent Guacci, and Douglas Koshland*
Department of Molecular and Cell Biology, University of California, Berkeley, Berkeley, CA 94720

ABSTRACT **Cohesin is a conserved protein complex required for sister chromatid cohesion, chromosome condensation, DNA damage repair, and regulation of transcription. Although cohesin functions to tether DNA duplexes, the contribution of its individual domains to this activity remains poorly understood. We interrogated the Smc3p subunit of cohesin by random insertion mutagenesis. Analysis of a mutant in the Smc3p hinge revealed an unexpected role for this domain in cohesion maintenance and condensation. Further investigation revealed that the Smc3p hinge functions at a step following cohesin's stable binding to chromosomes and independently of Smc3p's regulation by the Eco1p acetyltransferase. Hinge mutant phenotypes resemble loss of Pds5p, which binds opposite the hinge near Smc3p's head domain. We propose that a specific conformation of the Smc3p hinge and Pds5p cooperate to promote cohesion maintenance and condensation.**

Monitoring Editor
Kerry S. Bloom
University of North Carolina

Received: Aug 14, 2017
Revised: Nov 15, 2017
Accepted: Nov 20, 2017

INTRODUCTION

Cohesin is a conserved protein complex required for sister chromatid cohesion, chromosome condensation, DNA damage repair, and regulation of transcription (Onn *et al.*, 2008). To accomplish these functions, chromosome-bound cohesin tethers two distinct DNA duplexes or two sites on a single DNA duplex. A remarkable feature of cohesin-mediated tethers is that they must persist for long periods. For example, once generated, cohesion between sister chromatids must be maintained for up to several hours until cells progress through mitosis. Cohesion maintenance is essential for a successful mitosis since it ensures bipolar attachment and proper segregation of chromosomes. This process is crucial in mammalian oocytes since cohesion must be maintained from its establishment during meiotic prophase I, which occurs during fetal development, until the egg is fertilized in adulthood. Failure to maintain this cohesion can lead to aneuploidy and may cause infertility and birth defects in humans (Duncan *et al.*, 2012). However, despite its critical function, the mechanism and regulation of cohesion maintenance remains poorly understood.

Cohesin is a large multisubunit complex with an elaborate molecular architecture. In the budding yeast *Saccharomyces cerevisiae*, core cohesin subunits are Smc1p, Smc3p, Mcd1p (also called Scc1p), and Scc3p (Onn *et al.*, 2008). The Structural Maintenance of Chromosome (Smc) proteins fold back on themselves to form large dumbbell-shaped structures with two globular domains, referred to as the head and hinge, separated by an ~45-nm-long coiled coil (Onn *et al.*, 2008). Cohesin or purified Smc1p-Smc3p heterodimers have been visualized by electron microscopy, atomic-force microscopy, and scanning-force microscopy (Haering *et al.*, 2002; Sakai *et al.*, 2003; Kulemzina *et al.*, 2016). These studies revealed that Smc1p and Smc3p dimerize by an interaction between their heads and a separate interaction between their hinges. Dimerization of the heads is further stabilized by the kleisin subunit Mcd1p which binds through its N-terminus to Smc3p and its C-terminus to Smc1p (Haering *et al.*, 2002). The existence of two dimerization interfaces allows cohesin to form large rings. This ring structure likely explains cohesin's ability to bind DNA by topological entrapment. In addition to these ring structures, more complex conformations have also been observed (Sakai *et al.*, 2003). Evidence supporting the biological significance of these other conformations has been lacking.

Sister chromatid cohesion is established in S phase and then maintained until anaphase onset. Cohesion establishment is a multistep process. In budding yeast, the Scc2p/Scc4p complex

This article was published online ahead of print in MBoC in Press (http://www.molbiolcell.org/cgi/doi/10.1091/mbc.E17-08-0511) on November 29, 2017.

*Address correspondence to: Douglas Koshland (koshland@berkeley.edu).

Abbreviation used: DAPI, 4′,6-diamidino-2-phenylindole; EGTA, egtazic acid; FOA, 5-fluoroorotic acid; FRET, Förster resonance energy transfer; ORF, open reading frame; YPD, yeast extract, peptone, and dextrose.

(Ciosk *et al.*, 2000) loads cohesin onto DNA at centromeres and along chromosome arms at cohesin-associated regions (CARs) in early S phase (Megee *et al.*, 1999; Laloraya *et al.*, 2000; Glynn *et al.*, 2004). During S phase, DNA-bound cohesin is converted into a form that tethers sister chromatids by the Eco1p acetyltransferase, which acetylates Smc3p at lysines 112 and 113 (Skibbens *et al.*, 1999; Toth *et al.*, 1999; Rolef Ben-Shahar *et al.*, 2008; Ünal *et al.*, 2008; Zhang *et al.*, 2008). Once cohesion is established in S phase, the cohesion-associated regulator Pds5p is required to maintain cohesion until anaphase onset (Hartman *et al.*, 2000; Panizza *et al.*, 2000; Stead *et al.*, 2003).

The mechanism of cohesion maintenance is only partially understood. Pds5p colocalizes with cohesin on chromosomes and, when mutated, causes a decrease in cohesin binding to chromosomes, a reduction in cellular Mcd1p levels, and a cohesion maintenance defect (Hartman *et al.*, 2000; Panizza *et al.*, 2000). This maintenance defect can be suppressed by preventing premature Mcd1p degradation via a polySUMO-dependent pathway or preserving Smc3p acetylation by deleting the *HOS1* deacetylase (Stead *et al.*, 2003; Chan *et al.*, 2013; D'Ambrosio and Lavoie, 2014). Thus, Pds5p may function to protect cohesin complex from factors that could dissolve cohesion. However, cohesion maintenance is a more complex process. The cohesin mutant Mcd1-ROCC is defective for cohesion maintenance yet Mcd1p levels are not reduced and Pds5p recruitment to cohesin and chromosomes is unaffected (Eng *et al.*, 2014). These observations suggest that an additional step beyond Mcd1p stabilization or Pds5p recruitment is required for cohesion maintenance.

A clue for this additional step comes from imaging and biochemical studies of cohesin and Pds5p. Biochemical studies indicate Pds5p binds to Mcd1p, placing Pds5p adjacent to the Smc head domains (Chan *et al.*, 2013; Lee *et al.*, 2016; Muir *et al.*, 2016; Ouyang *et al.*, 2016). The functional significance of this interaction is supported by mutations in budding yeast Mcd1p that mimic the cohesion maintenance defects upon Pds5p depletion (Eng *et al.*, 2014). However, cross-linking has shown human Pds5Bp interacts with all cohesin subunits, implying that its association with cohesin is more extensive and/or dynamic (Huis in t Veld *et al.*, 2014; Hons *et al.*, 2016). Furthermore, in vivo Förster resonance energy transfer (FRET) suggested that Pds5p localizes near the hinge (Mc Intyre *et al.*, 2007) and atomic force microscopy shows Smc1p/Smc3p dimer conformations in which the hinge and head regions are adjacent (Sakai *et al.*, 2003). This proximity was supported by the observation that purified hinge domains are capable of binding to the head-associated Scc3p subunit of cohesin (Murayama and Uhlmann, 2015). Scc3p binds to the head and also binds Pds5p. Taken together these biochemical results suggest that cohesion might be maintained by an unanticipated conformation of cohesin involving binding of the hinge to the head.

Given the evidence that Pds5p has interactions with both the head and hinge regions, it is unclear how Pds5p mediates cohesion maintenance and which Smc domains are involved. To begin to address these issues, we conducted a comprehensive RID screen of Smc3p, a transposon-based mutagenesis approach that generates random five-amino-acid insertions. Here we characterize an insertion mutant located in the Smc3p hinge region. This mutant establishes cohesion but fails to maintain it, yet Pds5p remains bound to cohesin and to chromosomes. Previous work suggested that the Smc hinge region functions only in cohesion establishment (Gruber *et al.*, 2006; Kurze *et al.*, 2011). Our analysis reveals that the Smc3p hinge is important for cohesion maintenance.

RESULTS

The D667 region of the Smc3p hinge enhances but is not essential for cohesin binding at centromeres and cohesin-associated regions

We used a random insertion dominant (RID) screen to identify partial loss of function alleles of *SMC3* (Milutinovich *et al.*, 2007; Eng *et al.*, 2014, Orgil *et al.*, 2015). We expected to obtain RID screen mutations at the interfaces between Smc3p and Smc1p or Mcd1p. These mutations would be expected to prevent assembly and subsequent loading of cohesin onto chromosomes. In addition to assembly mutants, we predicted that mutations that preserved cohesin assembly would be found. We reasoned that if Smc3p function is modulated after cohesin assembles and binds chromosomes to maintain cohesion, then mutants of Smc3p could be found that impair this step.

Mutant *SMC3* alleles were generated by in vitro transposon-mediated mutagenesis, which produced a library encoding random five-amino-acid insertions (Supplemental Figure 1; see *Materials and Methods*). In this library, *SMC3* was placed under control of the conditional *pGAL1* promoter. The library was transformed into both wild-type haploid yeast and the temperature-sensitive *smc3-42* strain. Transformants were obtained on dextrose-containing media to repress RID library *pGAL1-SMC3* expression. Colonies were then screened for impaired growth on plates containing galactose as the carbon source to drive *pGAL1*-mediated overexpression of mutant *SMC3* alleles. The location of insertions within *SMC3* that impaired growth of wild-type (Supplemental Table 1) or *smc3-42* cells (Supplemental Table 2) when overexpressed were then determined by sequencing.

In the course of mapping RID mutations, we found 10 RIDs within the Smc3p hinge domain (Figure 1A). Nine of these RIDs were located near interfaces with Smc1p. Dimerization of the Smc1p and Smc3p hinges forms a toroidal structure with two interfaces termed "North" and "South" (Mishra *et al.*, 2010). Mutations that disrupt the hinge interfaces or that neutralize the positively charged amino acids in the central channel have been studied previously (Kurze *et al.*, 2011). Our screen identified three RIDs that mapped to the North hinge interface and six mapped near the South interface. Of the six RIDs near the South interface, five were located at or immediately adjacent to conserved glycine amino acids known to be necessary for SMC hinge dimerization in vitro (Figure 1B) (Hirano *et al.*, 2001). The sixth RID, encoding an insertion of five amino acids (AAAAD) following D667, maps to a hairpin loop extending from the top of a beta-sheet that contributes to the South hinge interface. We hypothesized that the unusual position of the D667 RID might reveal a novel function of the hinge in cohesin function.

The RID screen utilizes overexpression to generate a dominant phenotype. We wanted to determine whether *smc3-D667* could support viability when expressed at native levels. For this purpose, we transformed a haploid strain bearing *SMC3-3V5-AID* as the sole *SMC3*, henceforth abbreviated *SMC3-AID*, with either an integrating *smc3-D667* or *SMC3* wild-type allele under native expression at the *LEU2* locus. We then compared growth of the *SMC3-AID* parent alone to derivatives containing either *smc3-D667* or wild-type *SMC3*. Strains were grown to stationary phase in YPD then plated as 10-fold serial dilutions on YPD media alone or containing auxin. The auxin-inducible degron (AID) epitope on Smc3-AIDp allows its rapid and specific proteasome-mediated degradation when cells are treated with auxin (Nishimura *et al.*, 2009). As expected, the *SMC3-AID* parent is unable to grow on auxin-containing media, whereas the *SMC3* wild-type containing strain shows robust growth on auxin (Figure 1C). The *smc3-D667* containing cells failed to grow on

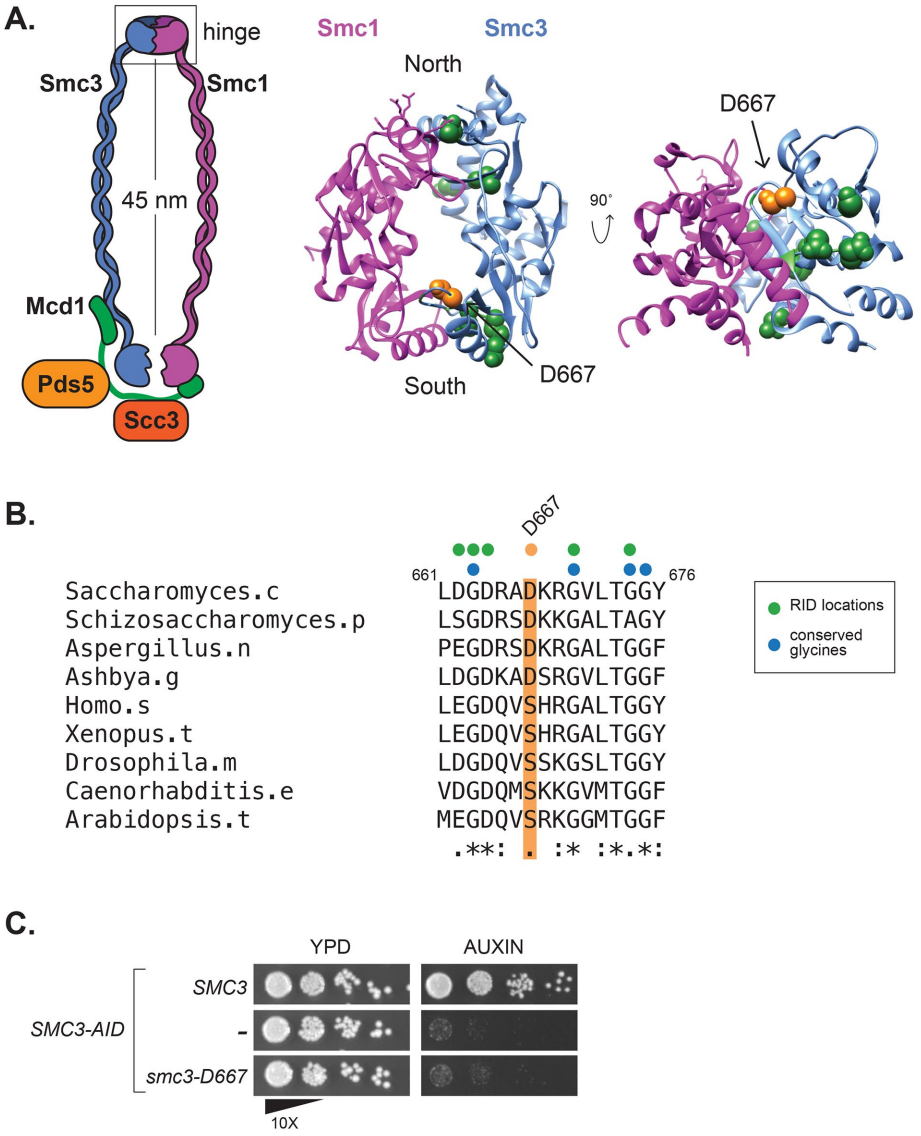

FIGURE 1: The *smc3-D667* RID mutation maps to a loop near the South interface of the Smc3p hinge. (A) Diagram of cohesin highlighting location of the *smc3-D667* RID insertion. The homologous residue of *smc3*-D667, highlighted in orange, was determined by sequence alignment using ClustalW and mapped onto the mouse Smc1p/Smc3p hinge crystal structure (PDB: 2WD5; Kurze *et al.*, 2011). Other RIDs isolated in this screen and located in the hinge domain are represented as green spheres, and their positions were also approximated by sequence alignment. (B) Sequence alignment of Smc3p homologues showing the conserved region around D667. The position of Asp667 is highlighted in orange, and the sequence of the five-amino-acid insertion, AAAAD, that follows Asp667 in the *smc3-D667* RID is depicted above as an orange dot. The position of other RIDs in this region are shown with green dots and conserved glycine residues shown with blue dots. (C) The *smc3-D667* allele under the native *SMC3* promoter is unable to support viability. Cultures of haploid strains *SMC3 SMC3-AID* (BRY474), *SMC3-AID* (VG3651-3D), and *smc3-D667 SMC3-AID* (BRY482) were grown to saturation in YPD and then plated in 10-fold serial dilutions onto YPD alone (YPD) or containing 0.75 mM auxin (auxin) and then grown for 2 d at 23°C.

media containing auxin. The fact that *smc3-D667 SMC3-AID* cells grew well in the absence of auxin indicated that *smc3-D667* is recessive unless overexpressed. The *smc3-D667* mutant may fail to support viability on auxin because it disrupts the sequence of charged amino acids that follow D667. Therefore, we assessed the viability of two *SMC3* alleles in which D667 and nearby charged amino acids had been mutated to alanine. Unlike the *smc3-D667* RID mutant, the *smc3-D667A* single mutant and the *smc3-D667A,K668A,R669A* triple mutant supported growth of *SMC3-AID* cells on auxin (Supplemental Figure 1B). Therefore, the *smc3-D667* RID likely disrupted Smc3p function independent of its effect on nearby charged amino acids. In summary, the *smc3-D667* RID allele was unable to support one or more essential cohesin functions.

The inviability of *smc3-D667* cells could be due to a failure of cohesin to bind DNA or a failure to perform an essential cohesin function after binding DNA. To distinguish between these possibilities, we first assessed whether smc3-D667p cohesin binds DNA. Strains containing *SMC3-AID* alone or also a second *SMC3*, either wild-type *SMC3* or *smc3-D667*, were arrested in G1 phase and treated with auxin to deplete Smc3-AIDp. Cells were then synchronously released from G1 into YPD media containing auxin and nocodazole to rearrest them in mid–M phase while maintaining Smc3-AIDp depletion (Figure 2A and *Materials and Methods*). To assess qualitatively whether *smc3-D667* supported binding of cohesin to chromosomes, we processed mid–M phase–arrested cells for chromosome spreads and assessed chromosomal binding of the cohesin subunit Mcd1p by immunofluorescence. Mcd1p is a marker for the cohesin complex, since Mcd1p cannot bind chromosomes unless it is part of the four-subunit complex (Toth *et al.*, 1999). As expected, robust Mcd1p signal was observed on chromosome spreads from cells with Smc3p (*SMC3 SMC3-AID*) but not from cells without it (*SMC3-AID*) (Figure 2B). In *smc3-D667 SMC3-AID* cells, Mcd1p bound to chromosomes at levels similar to wild-type cells. This result indicated that smc3-D667p supports both cohesin complex assembly and binding to chromosomes.

We used chromatin immunoprecipitation (ChIP) to assess whether the cohesin chromosomal binding observed via spreads reflected specific binding to CARs and centromeres. Mid–M phase cells prepared as described for chromosome spreads (Figure 2A) were fixed and processed for ChIP (Figure 2A and *Materials and Methods*). Cohesin binding was assessed using anti-Mcd1p antibodies. As expected, Mcd1p binding to CARs and centromeres was robust in cells with Smc3p (*SMC3 SMC3-AID*) and absent in those without it (*SMC3-AID*) (Figure 2C). Mcd1p binding in *smc3-D667* cells was similar to wild type at centromeres (Figure 2C, right) and at the pericentromeric *CARC1* peak (Figure 2C, left) but somewhat reduced at centromere-distal *TRM1* and *CARL1* peaks (Figure 2C, center, and Supplemental Figure 2A). These results indicated that smc3-D667p cohesin localizes to CARs and centromeres. To corroborate further the DNA binding of smc3-D667p, we generated strains bearing Smc3p and smc3-D667p

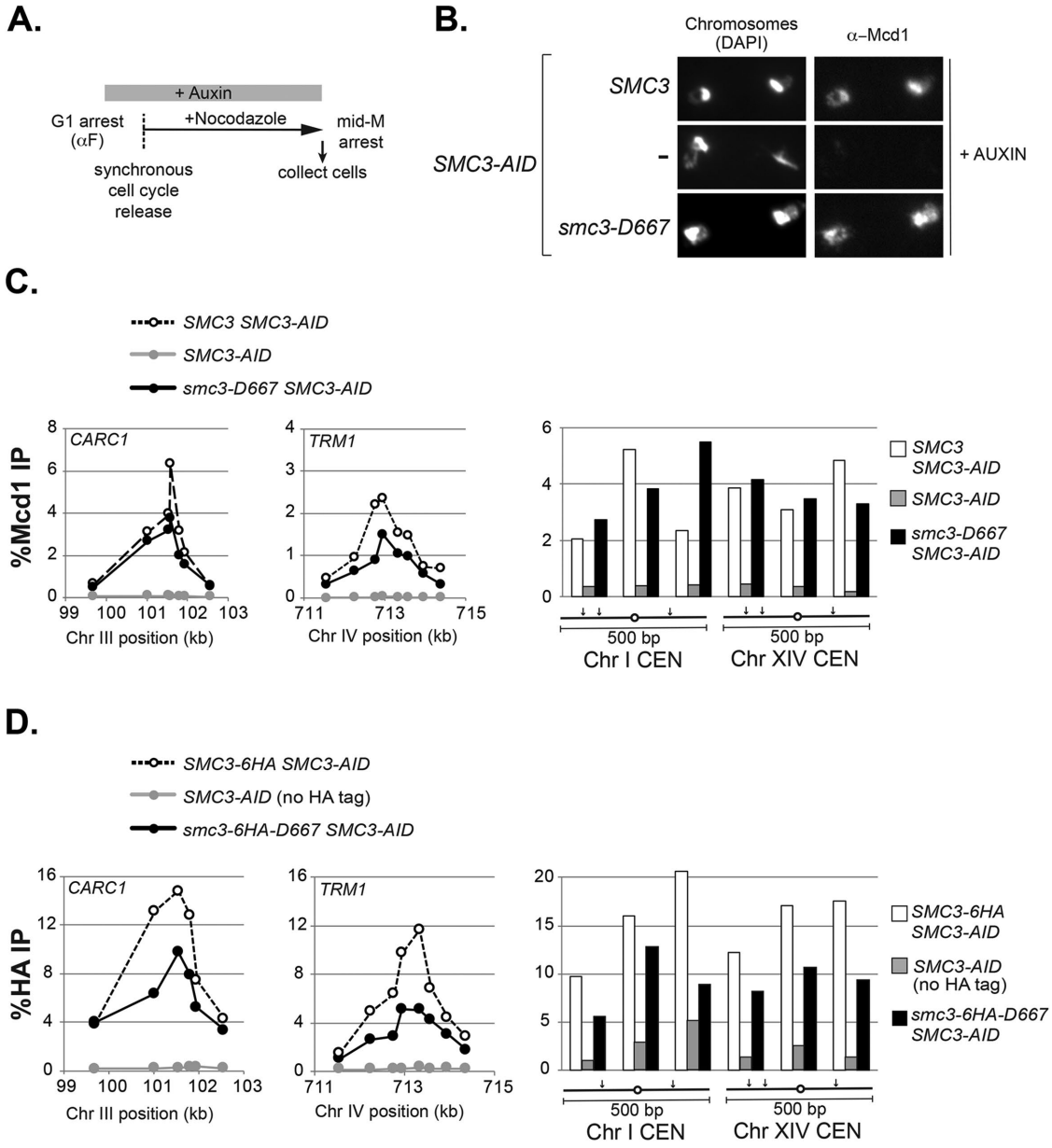

FIGURE 2: Cohesin containing smc3-D667p binds to chromosomes in mid–M phase–arrested cells. (A) Regimen used to prepare cells synchronously arrested in mid–M phase. Cultures were grown to mid–log phase at 23°C and treated with alpha factor for 3 h to arrest cells in G1 phase and then auxin was added and cells were incubated an additional hour in G1 to deplete Smc3-3V5-AIDp. Cells were synchronously released from G1 arrest into YPD media containing auxin and nocodazole to re-arrest in mid–M phase (*Materials and Methods*). (B) Chromosome spreads showing that smc3-D667p cohesin binds chromosomes at levels similar to wild type. Haploid *SMC3 SMC3-AID* (BRY474), *SMC3-AID* (VG3651-3D), and *smc3-D667 SMC3-AID* (BRY482) cells were grown as described in A. Aliquots of mid–M phase–arrested cells were fixed and processed for chromosome spreads. Bulk chromosomal DNA (DAPI) and cohesin binding (α–Mcd1) are shown. (C, D) ChIP showing that *smc3-D667* cohesin binds to CARs and centromeres. (C) Haploid strains in B were arrested in mid–M phase as described in A and then fixed and processed for ChIP as described under *Materials and Methods*. ChIP of Mcd1p binding at *CARC1* (left) and *TRM1* (middle) and at two centromeres (right). Wild-type strain *SMC3* (dotted lines and white bars), *smc3-D667* strain (black lines and black bars), and *SMC3-AID* alone (gray lines and gray bars). (D) ChIP of HA epitope tagged Smc3p and smc3-D667p at *CARC1* (left), *TRM1* (middle), and at two centromeres (right). Haploid strains *SMC3-6HA SMC3-AID* (BRY604; dotted lines and white bars), *smc3-6HA-D667 SMC3-AID* (BRY602; black lines and black bars) and *SMC3-AID* only (VG3651-3D; gray lines and gray bars) were arrested and processed for ChIP as described in C.

tagged with a 6HA epitope in the *SMC3-AID* background. Mid–M phase auxin-treated cells were prepared (Figure 2A) and the presence of smc3-6HA-D667 and Smc3-6HAp were confirmed by Western blotting (Supplemental Figure 3). We then performed ChIP using anti-HA to directly monitor the Smc3p cohesin subunit. As was observed in the Mcd1p ChIP, smc3-6HA-D667p (*smc3-6HA-D667 SMC3-AID*) bound to CARs and centromeres, albeit at levels 50% reduced relative to wild-type Smc3p (Figure 2D and Supplemental

Figure 2B). These data, using two different cohesin subunits, show that smc3-D667p cohesin complex binds to CARs and centromeres at ~50% the levels of wild type.

The D667 region of the Smc3p hinge is required to maintain cohesion

Smc3-D667p cohesin binds chromosomes, so we assayed whether it can perform cohesin's function of tethering sister chromatids. Therefore, we assessed sister chromatid cohesion at centromere-proximal (*TRP1)* or centromere-distal (*LYS4*) loci by integrating tandem LacO repeats in strains that express a GFP-LacI fusion (Figure 3A and *Materials and Methods*). Strains bearing *SMC3-AID* alone or also containing either wild-type *SMC3* or *smc3-D667* were arrested in G1, treated with auxin to degrade Smc3-AIDp, and then synchronously released from G1 into media containing auxin and nocodazole to allow progression through S phase and arrest in mid–M phase (Figure 2A). Nearly all G1 cells in all strains contained a single GFP focus, indicating no preexisting aneuploidy (Figure 3B). As expected, only a small fraction of mid–M phase–arrested cells with Smc3p (*SMC3 SMC3-AID*) lost cohesion at *TRP1* or *LYS4*, whereas cells lacking Smc3p (*SMC3-AID*) had almost complete loss of cohesion. Nearly two-thirds of cells expressing only *smc3-D667* (*smc3-D667 SMC3-AID)* also had lost cohesion at these two loci. This result suggested that the D667 region of the hinge was required for either robust establishment and/or maintenance of cohesion.

These two possibilities can be distinguished by kinetic analysis of cohesion in populations of cells synchronously progressing through the cell cycle. Mutants that compromise cohesion establishment like those defective in core subunits of cohesin *MCD1*, *SMC3,* and *SMC1* exhibit sister chromatid separation immediately after DNA replication (Guacci *et al.*, 1997; Michaelis *et al.*, 1997). Mutants that compromise cohesion maintenance like those defective in the cohesin regulator *PDS5* also lose cohesion but significantly later in the cell cycle than establishment mutants (Tanaka *et al.*, 2001; Stead *et al.*, 2003; Noble *et al.*, 2006; Eng *et al.*, 2014). Using the same strains as described above along with a *PDS5-AID* strain, we assessed when cohesion was lost in *smc3-D667*. Strains were arrested in G1 and treated with auxin to degrade Smc3-AIDp and then released from G1 in the presence of auxin and nocodazole to allow cells to progress through S phase and arrest in mid–M. After release from G1, aliquots of cells were removed every 15 min to assess DNA content and cohesion at *TRP1* and *LYS4* (Figure 3C).

From analysis of the DNA content, all strains exhibited nearly identical kinetics of progression through S phase and subsequent arrest in mid–M (Supplemental Figure 4A). As expected for cells expressing Smc3p (*SMC3 SMC3-AID*), sister chromatids were paired through mid–M arrest, so few cells with separated sisters were detected. In contrast, both strains lacking Smc3p (*SMC3-AID*) and Pds5p (*PDS5*-AID) lost cohesion. However, the cohesion loss in the *PDS5-AID* cells was delayed by ~20 min, as published previously (Eng *et al.*, 2014). Cells expressing only smc3-D667p (*smc3-D667 SMC3-AID*) resembled *PDS5-AID* cells, with delayed cohesion loss at the *LYS4* locus and a more pronounced delay in cohesion loss at the *TRP1* locus. This delay in cohesion loss in cells with smc3-D667p demonstrated that *smc3-D667* cells, like Pds5p-deficient cells, could establish but not maintain cohesion. Thus, the D667 region of the Smc3p hinge is important specifically for efficient maintenance of cohesion at both *CEN*-proximal and *CEN*-distal loci.

Cohesin is required to recruit the maintenance factor Pds5p to chromosomes (Hartman *et al.*, 2000; Panizza *et al.*, 2000). Since cells expressing smc3-D667p displayed a cohesion maintenance defect identical to cells depleted of Pds5p, we tested whether smc3-D667p cohesin was able to recruit Pds5p to chromosomes. To address this possibility, we first analyzed whether smc3-D667p supported Pds5p binding to chromosomes by ChIP using a Pds5p antibody (Figure 3D and Supplemental Figure 4B). The ratio of Pds5p bound to CARs and centromeres in cells with smc3-D667p (*smc3-D667 SMC3-AID*) to Smc3p was very similar to that seen for Mcd1p or smc3-6HA-D667p. These results indicate that cohesin with smc3-D667p can bind Pds5p and recruit it to chromosomes. The ability of Pds5p to bind cohesin with smc3-D667p was then tested by coimmunoprecipitation (Figure 3E). Cells expressing FLAG-tagged Scc3p and HA-tagged Smc3p or smc3-D667p were arrested in M-phase after auxin-mediated depletion of Smc3-AIDp. Scc3p was immunoprecipitated using anti-FLAG antibody and cohesin subunits detected in the precipitates by Western blot. As expected, no Pds5p was detected in the FLAG immunoprecipitate from cells lacking Smc3p or when Scc3p was untagged (first and second lanes), while Pds5p and Smc3-6HAp were detected in the immunoprecipitate from cells expressing Smc3-6HAp (third lane). Importantly, similar Pds5p levels were observed in the immunoprecipitate from cells expressing smc3-D667-6HAp (fourth lane). Thus, smc3-D667p cohesin binds Pds5p and recruits it to DNA.

The D667 region of the Smc3p hinge is not required for its stable binding to chromosomes

Cohesin is known to convert from a DNA-bound, untethered state to a tethered state in S phase (Rolef Ben-Shahar *et al.*, 2008; Ünal *et al.*, 2008). We envisioned two models by which cohesion that had been established in S phase by smc3-D667p could fail to be maintained as cells progressed into M phase. In one model, cohesin reverts back to its untethered state without perturbing cohesin binding to DNA. Precedence for this phenotype comes from the cohesin mutant *mcd1-ROCC* which, like *smc3-D667*, is defective for cohesion maintenance (Eng *et al.*, 2014). Alternatively, the smc3-D667p is less stably bound so dissociates from DNA. In this model, following cohesion establishment, cohesin dissociation from chromosomes could manifest as a cohesion maintenance defect. Detecting putative cohesin dissociation is difficult, because the Scc2p/Scc4p complex continues loading cohesin onto chromosomes in mid–M phase creating a pool of bound cohesin that does not contribute to cohesion (Lengronne *et al.*, 2006). Therefore, the Scc2p/Scc4p complex must be inactivated to allow detection of cohesin dissociation.

To distinguish between these two models, we examined the stability of smc3-6HA-D667p binding to DNA under conditions where additional loading was prevented by depletion of the cohesin loader subunit Scc2p. This loader depletion approach revealed that in wild-type cells, cohesin (Mcd1p) binds stably at CARs but exhibits reduced stability at centromeres (Eng *et al.*, 2014). Therefore, we replaced *SCC2* with *SCC2-3FLAG-AID* in *SMC3-AID* strains bearing either wild-type Smc3-6HAp or smc3-D667-6HAp. Cultures of these strains were grown to mid–log phase and arrested in mid–M phase by addition of nocodazole. Cultures were then split and either auxin or vehicle (DMSO) was added, and then they were incubated for 1 h. The aliquot containing auxin will deplete both Scc2-3FLAG-AIDp and Smc3-3V5-AIDp. Samples were collected and either fixed for ChIP or processed for Western blot analysis (Figure 4A). Depletion of Scc2-3FLAG-AIDp and Smc3-3V5-AIDp was confirmed by Western blot (Figure 4B).

ChIP of Smc3-6HAp showed no difference in binding to CAR peaks *TRM1* and *CARL1* after Scc2-3FLAG-AIDp depletion (Figure 4C, left). The persistence of high ChIP levels even after 1 h indicated that cohesin remained very stably bound to DNA. Similarly, smc3-6HA-D667p ChIP at *TRM1* and *CARL1* peaks was unchanged by

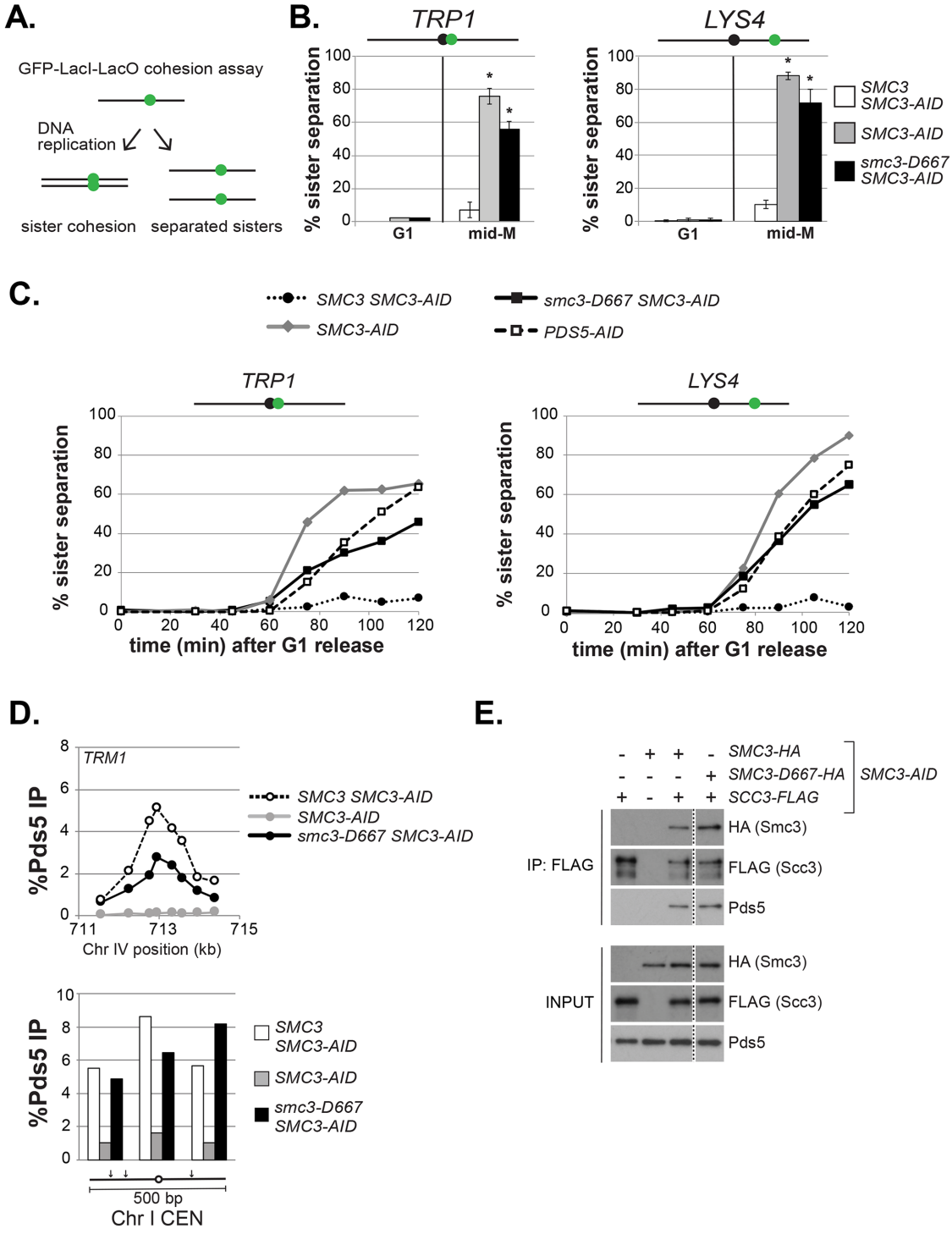

FIGURE 3: The *smc3-D667* mutant exhibits a cohesion maintenance defect. (A) Schematic of cohesion loss assay using loci tagged with GFP-LacI. After replication, cells with cohesion have a single GFP focus, whereas cells where cohesion is lost have two GFP foci. (B) Cohesion loss at *CEN*-proximal *TRP1* and *CEN*-distal *LYS4* loci in mid–M phase–arrested cells. Haploid strains were arrested in G1, depleted of Smc3p-AID, and then synchronously released from G1 and rearrested in mid–M phase under depletion conditions as described in Figure 2A. LacO arrays integrated at *TRP1* (left) in haploid *SMC3-AID* yeast alone (BRY676) or also containing wild-type *SMC3* (BRY678) or *smc3-D667* (BRY680). LacO arrays integrated at *LYS4* (right) in *SMC3-AID* yeast alone (VG3651-3D) or containing wild-type *SMC3* (BRY474) or *smc3-D667* (BRY482). Samples were collected from G1-arrested auxin-treated cells and mid–M phase–arrested cells and scored for cohesion. The percentage of cells with two GFP foci (sister separation) were averaged from two independent experiments and plotted. Cells (100–200) were scored per sample at each time point. Error bars represent SD. *$p < 0.05$ when tested against *SMC3 SMC3-AID* % sister separation in mid–M (*t* test, two-tailed). (C) Time course to assess the kinetics of cohesion loss. Haploid strains were arrested in G1, treated with auxin, and synchronously released into mid–M phase arrest in auxin containing media as described in Figure 2A. Samples were collected in G1 and every

Scc2-3FLAG-AIDp depletion (Figure 4C, right). At centromeres, Smc3-6HAp shows somewhat reduced binding after Scc2-3FLAG-AIDp depletion, confirming that this cohesin is less stably bound. Similarly, somewhat reduced binding of smc3-6HA-D667p to centromeres was observed. These results demonstrated that smc3-6HA-D667p was as stably bound to chromosomes as wild-type Smc3-6HAp. Importantly, our results indicated that in mid–M phase–arrested *smc3-D667* cells, when most sister chromatid cohesion is lost (Figure 3), smc3-D667p cohesin is stably bound to chromosomes. Thus, the D667 region of the Smc3p hinge performs a function in maintaining cohesion other than ensuring stable binding to DNA.

The D667 region of the Smc3p hinge modulates cohesion and supports viability by a mechanism independent of Eco1p-dependent acetylation

Eco1p is necessary for establishing cohesion during S phase through its acetylation of Smc3p at lysines K112 and K113. Although cohesion establishment occurs during S phase, Smc3p acetylation remains until anaphase onset, suggesting it may be required to maintain cohesion (Beckouet *et al.*, 2010). Since smc3-D667p supported cohesion establishment, we predicted that it would be acetylated by Eco1p. Therefore, we used an antibody that specifically recognizes acetylated Smc3p-K113 to test the acetylation of smc3-D667p in cells arrested in mid–M. Cells were arrested in mid–M after auxin depletion (Figure 5A). As expected, in cells depleted of Eco1-AIDp or Smc3-AIDp, no acetylated Smc3p was detected (Figure 5B). While wild-type Smc3p showed a strong acetylation signal, acetylation signal for smc3-D667p was reduced. A reduction in acetylation signal was expected because cohesin was known to be acetylated only after binding to DNA, and less cohesin with smc3-D667p was bound to DNA than wild-type cohesin (Figure 2). Direct comparison of acetylation levels is possible when signal from the acetylation-recognizing antibody is linear across the observed range. However, we found that signal from the acetylation antibody was nonlinear (Supplemental Figure 5), making it possible that smc3-D667p acetylation levels were closer to Smc3p than Figure 5B suggested.

To assess whether the reduced amount of smc3-D667p acetylation was responsible for the cohesion maintenance defect, we first asked whether a change in acetylation levels correlated with the appearance of the cohesion defect. Reduced smc3-D667p acetylation may have resulted from a failure to acetylate it in S phase or to maintain it after S phase. To distinguish between these possibilities, we immunoprecipitated smc3-6HA-D667p from cells progressing synchronously through S phase following release from G1 arrest (Figure 5C). As expected, wild-type Smc3-6HAp acetylation began to appear during S phase and then increased and remained high through M phase arrest (Figure 5D). While acetylation of smc3-6HA-D667p was lower than WT in early S phase, it increased as cells progressed into M phase. Therefore, *smc3-D667* cells establish cohesion with low smc3-D667p acetylation levels, but its failure to maintain cohesion is not due to a subsequent decrease in acetylation levels.

We further examined the correlation between Smc3p acetylation levels and cohesin function by asking whether low levels of Smc3p acetylation always led to loss of essential cohesin function. Temperature-sensitive *eco1* mutants (*eco1-203* and *eco1-1*) establish and maintain cohesion at permissive temperature, yet *eco1-1* has greatly reduced acetylation (Toth *et al.*, 1999; Heidinger-Pauli *et al.*, 2009; Rowland *et al.*, 2009). We therefore compared Smc3p acetylation levels of the *eco1-203* mutant grown at the permissive temperature 23°C to the *smc3-D667* mutant. The level of Smc3p acetylation in *eco1-203* cells was very similar to *smc3-D667* cells (Figure 5E). This result suggested that the level of smc3-D667p acetylation was sufficient to support cohesion function. However, we could not rule out that the acetylation level of smc3-D667p was below a critical threshold too subtle to distinguish by Western blot.

We sought additional support for the idea that the lower smc3-D667p acetylation level is not responsible for its mutant phenotype. For this purpose, we assayed the *smc3-D667* mutant in the *SMC1-D1164E* mutant background, as this *SMC1* allele completely bypasses the need for Smc3p acetylation in both cohesion and viability (Çamdere *et al.*, 2015; Elbatsh *et al.*, 2016). In the presence of auxin, *smc3-D667 SMC3-AID* and *SMC1-D1164E smc3-D667 SMC3-AID* cells were inviable (Figure 6A). Therefore, the viability defect of *smc3-D667* is distinct from *eco1-ts* and deletion mutants, which are bypassed by *SMC1-D1164E*. We next asked whether *SMC1-D1164E* restored cohesion to *smc3-D667* cells as was observed for the *eco1*Δ *wpl1*Δ mutant and *eco1*Δ cells (Çamdere *et al.*, 2015). As expected, *SMC1-D1164E* restored cohesion at the *LYS4* locus in the *eco1*Δ *wpl1*Δ mutant (Figure 6B and Çamdere *et al.*, 2015). However, *SMC1-D1164E* failed to restore cohesion to the *smc3-D667 SMC3-AID* mutant in the presence of auxin (Figure 6C). These results supported the idea that the viability and cohesion defects of *smc3-D667* cells were independent of reduced levels of Smc3p acetylation.

The D667 region of the Smc3p hinge is required for *rDNA* condensation and viability even in the absence of antagonism by Wpl1p

In addition to sister chromatid cohesion, cohesin and its regulators Pds5p and Eco1p are required for the proper mitotic condensation

15 min starting 30 min after G1 release and fixed to assess cohesion loss and DNA content. Data are shown as the percentage of cells with separated sisters. Cells (100–200) were scored for cohesion for each time point. DNA content was assessed by flow cytometry and shown in Supplemental Figure 4A. The left side shows cohesion loss at the *CEN*-proximal *TRP1* locus. Haploid strains *SMC3 SMC3-AID* (BRY678), *SMC3-AID* (BRY676), *smc3-D667 SMC3-AID* (BRY680), and *PDS5-AID* (BRY815). The right side shows cohesion loss at the *CEN*-distal *LYS4* locus. Haploid strains *SMC3 SMC3-AID* (BRY474), *SMC3-AID* (VG3651-3D), *smc3-D667 SMC3-AID* (BRY482), and *PDS5-AID* (TE228). (D) ChIP to assess Pds5p binding to chromosomes. Haploid strains *SMC3 SMC3-AID* (BRY474), *SMC3-AID* (VG3651-3D), and *smc3-D667 SMC3-AID* (BRY482) arrested in mid–M phase according to the regimen in Figure 2A were fixed and processed for ChIP using polyclonal anti-Pds5p antibody. Pds5p binding was assessed at the CAR *TRM1* (top), and centromeres I and XIV (bottom). (E) Smc3-D667p supports assembly of cohesin containing Pds5p and Scc3-3FLAGp. Haploid strains *SMC3-AID* (VG3561-3D), *SCC3-3FLAG SMC3-AID* (BRY607), *SMC3-6HA SMC3-AID* (BRY604), *SCC3-3FLAG SMC3-6HA SMC3-AID* (BRY621), and *SCC3-3FLAG smc3-6HA-D667 SMC3-AID* (BRY625) cells were grown as described in Figure 2A. Protein extracts were made and Scc3p immunoprecipitated using anti-FLAG antibody, subjected to SDS–PAGE and Western blot analysis using the indicated antibodies. Dotted line indicates where an irrelevant lane was removed.

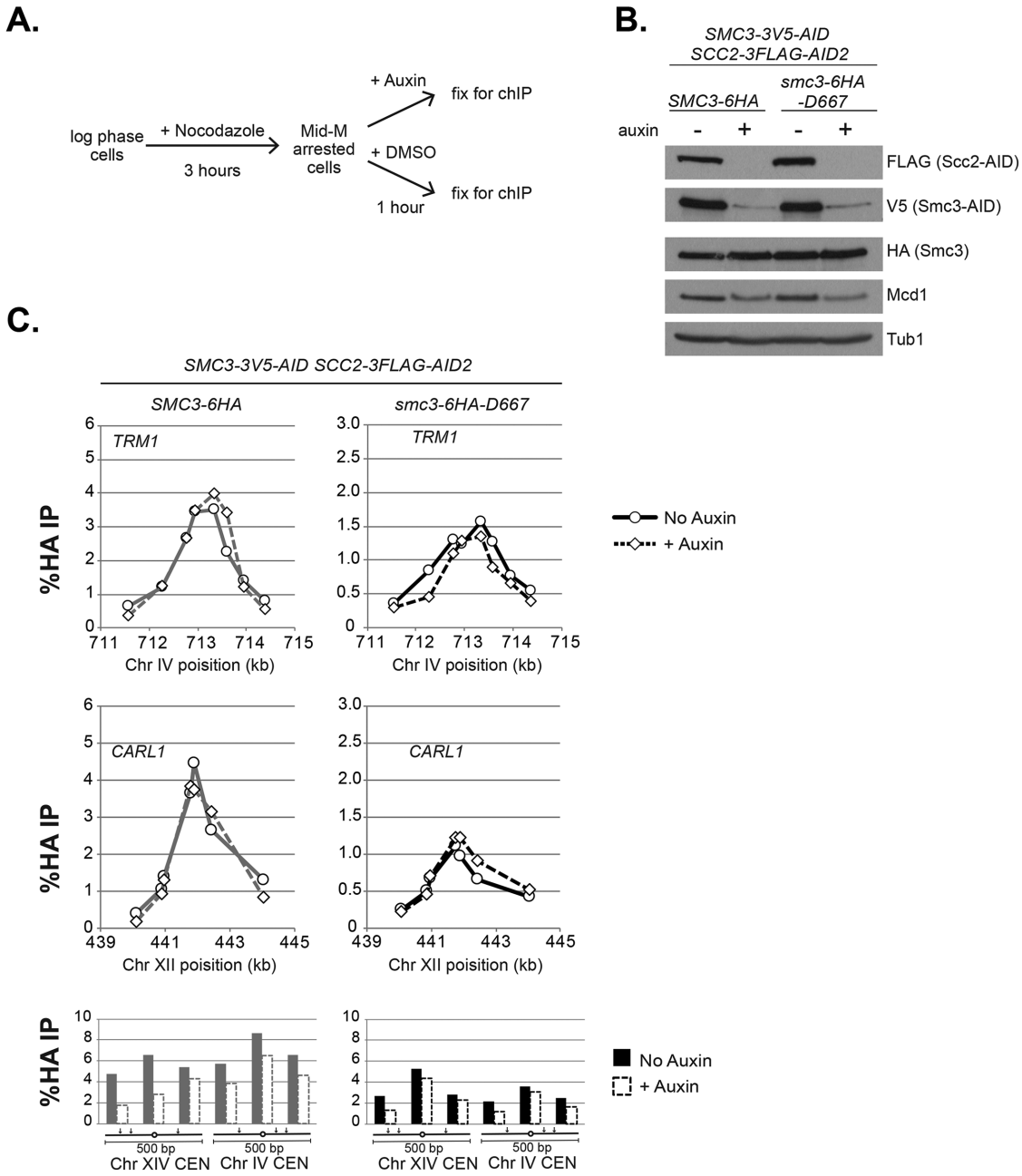

FIGURE 4: *smc3-D667* supports stable cohesin binding to chromosomes. (A) Regimen used to assess stability of cohesin binding to DNA on depletion of the loader subunit Scc2p. Haploid *SMC3-3V5-AID SCC2-3FLAG-AID2* strains expressing either *SMC3-6HA* (BRY839) or *smc3-6HA-D667* (BRY841) were grown to mid–log phase and arrested in mid–M phase by incubation with nocodazole for 3 h. Cultures were split, and auxin added to one half, and then both halves were incubated for 1 h. Cells aliquots were collected to make protein extracts or fixed and processed for ChIP (*Materials and Methods*). (B) Western blot analysis showing depletion of AID-tagged proteins. Protein extracts (TCA lysed) of strains in A were subjected to SDS–PAGE and analyzed by Western blot. Depletion of Scc2p-3FLAG-AID (FLAG) and Smc3p-3V5-AID (V5) is shown. Antibodies assessing levels of Smc3p (HA) and Mcd1p (Mcd1) cohesin subunits and a loading control (Tub1). (C) ChIP to assess the stability of cohesin (Smc3p) binding at CARs and centromeres. Cultures of strains from A were fixed and processed for ChIP. Smc3-6HAp binding (left side) and smc3-6HA-D667p binding (right side) at CARs and centromeres in control cells (solid lines and filled columns) and auxin-treated cells depleted for Scc2-3FLAG-AID2p and Smc3-3V5-AIDp (dashed lines and open columns). From top to bottom: binding to CARs *TRP1* and *CARL1*, and centromeres XIV and IV.

of chromatids in budding yeast (Guacci *et al.*, 1997; Skibbens *et al.*, 1999; Hartman *et al.*, 2000). We addressed whether *smc3-D667* cells supported condensation by examining the morphology of the *rDNA* locus on chromosome XII. In chromosome spreads the *rDNA* is located on the periphery of the primary chromosome mass. In interphase, the *rDNA* can be seen as a diffuse puff while in M phase it condenses into a loop (Guacci *et al.*, 1994). Chromosome spreads of the *SMC3-AID* and *PDS5-AID* strains were prepared from cells

arrested in mid–M phase (Figure 7A). The *rDNA* morphology was scored as 1) a tight, fully condensed loop; 2) a wide, decondensed loop; or 3) diffuse, with no apparent loop. In cells with wild-type Smc3p, the *rDNA* formed tight loops in almost all chromosome masses, indicative of chromosome condensation. In cells lacking Smc3p (*SMC3-AID*), the *rDNA* was almost always present as a diffuse mass, recapitulating the established role of Smc3p and cohesin in condensation. Cells expressing only smc3-D667p or depleted of Pds5p (*PDS5-AID*) exhibited very similar condensation defects and tight loops were rarely observed (Figure 7A). Thus, the D667 region of the Smc3p hinge is needed for two M-phase functions of cohesin, the maintenance of cohesion and condensation.

We next asked whether the condensation defect and inviability of *smc3-D667* cells was due to antagonism by Wpl1p. Deletion of *WPL1* restores viability to *eco1* temperature-sensitive or *eco1*Δ strains that have impaired or absent acetylation (Rowland *et al.*, 2009; Guacci and Koshland 2012). If the defect of *smc3-D667* can be attributed to a loss of Eco1p function, then *wpl1*Δ would restore condensation and viability to *smc3-D667* cells. To test this idea, we characterized the consequences of *WPL1* deletion in the *smc3-D667* strain. *wpl1*Δ failed to restore viability to *smc3-D667 SMC3-AID* cells on media containing auxin (Figure 7B). Consistent with *smc3-D667* representing a defect distinct from cells lacking Smc3p acetylation, *wpl1*Δ failed to restore condensation of the *rDNA* or cohesion to *smc3-D667* cells (Figure 7, C and D, respectively). Altogether, our observations confirmed that the critical defects in *smc3-D667* cells were independent of Smc3p acetylation or antagonism by Wpl1p.

The D667 region is necessary for interallelic complementation

Interallelic complementation between alleles of *SMC3* or *MCD1* revealed the ability of two separate cohesin complexes to share activities to restore cohesin functions. Additional evidence suggests that this communication between cohesins might reflect direct cohesin–cohesin interaction on chromosomes (Eng *et al.*, 2015). We wondered whether the D667 region of the hinge was needed for cohesin–cohesin communication. To test this idea, we asked whether *smc3-D667* could partner with the temperature-sensitive *smc3-42* allele to exhibit interallelic complementation. The temperature-sensitive *smc3-42* strain cannot grow at its restrictive temperature of 34°C. Previously it had been shown that the *smc3-K113R* allele cannot support viability as the sole copy of *SMC3*. However, a strain in which both *smc3-K113R* and *smc3-42* alleles are present exhibits robust growth at 34°C, a condition in which neither single mutant can grow (a summary of complementation relationships is provided in Figure 8B). With this knowledge, we asked whether *smc3-D667* could substitute for *smc3-K113R* and complement *smc3-42*. As a metric for the extent of interallelic complementation, we repeated the previous experiment with *smc3-42* and *smc3-K113*. As expected, at 34°C neither *smc3-42* nor *smc3-K113R* single mutants were viable, while the *smc3-42 smc3-K113R* double mutant showed robust growth similar to wild type (Figure 8A). As expected, the *smc3-D667* single mutant failed to grow. The double *smc3-42 smc3-D667* mutant resembled the growth of *smc3-42* alone. Thus, the property of interallelic complementation observed between *smc3-42* and *smc3-K113R* was not observed between *smc3-42* and *smc3-D667*. Therefore, *smc3-D667* lacks the activity necessary for interallelic complementation. This result suggested that the D667 region of the hinge is necessary for cohesin–cohesin communication.

DISCUSSION

Cohesin has a complex architecture with a heterodimeric ATPase domain and a hinge domain connected by a long coiled coil. The roles of these domains in cohesin's activity on chromosomes is poorly understood. Here, we identified and characterized *smc3-D667*, a mutant in the Smc3p hinge domain that blocks cohesin function in M phase. Kinetic analyses of cohesion during the cell cycle reveal that this mutation allows cohesion establishment but impairs subsequent maintenance of cohesion. We also show that this mutation impairs mitotic chromosome condensation of the *rDNA*. However, this mutation does not perturb the stable association of cohesin with chromosomes as measured by the persistence of this association even after loader inactivation. Together, our results support a function of cohesin's hinge domain in cohesion maintenance and condensation independent of cohesin's stable binding to chromosomes.

The cohesion maintenance and condensation functions of the hinge domain revealed by *smc3-D667* have not been reported previously. Two mutations that impact the North and South interfaces of the hinge dimer revealed a role of the hinge in cohesin binding to chromosomes, as expected given the role of the hinge dimer in maintaining the topological integrity of cohesin (Mishra *et al.*, 2010). The novel phenotypes of *smc3-D667* are consistent with D667 localization, determined by alignment to Smc3p homologues, within a loop not expected to impact the dimer interface. One study designed a cluster of mutations in *SMC1* and *SMC3* that neutralize the positive charges in a central channel formed by hinge dimerization (Kurze *et al.*, 2011). This cluster of mutations (charge neutralization alleles) caused defects in cohesion and Smc3p acetylation but did not impair stable binding of cohesin to chromosomes, all phenotypes similar to the *smc3-D667* allele. However, unlike our study of *smc3-D667,* the charge neutralization alleles were not analyzed for establishment and maintenance of cohesion, the functional significance of the reduced Smc3p acetylation, or condensation. If these alleles had the same cohesion and condensation defects as the *smc3-D667* allele, as we predict, then these results would imply that changes to two distinct regions of the hinge dimer contribute to a common function needed for cohesion maintenance and condensation. The potential cooperation of the D667 region of the Smc3p hinge and the hinge channel could reflect a previously unrecognized conformational change of the hinge dimer needed for cohesin function. Indeed, in addition to the strict toroidal structures seen by crystallization of the cohesin or *Tm*SMC hinge dimers, a recently published structure of the related *Gs*SMC hinge dimer revealed that hinge dimers may adopt an asymmetric, relaxed conformation resembling a spring washer (Haering *et al.*, 2002; Kurze *et al.*, 2011; Kamada *et al.*, 2017). Surprisingly, while both hinge interfaces remained intact in this structure, the relaxed face of the GsSMC hinge dimer involved a break in the beta-sheet connected by a loop homologous to the D667 loop of Smc3p. Together with our results, further investigation of hinge structural flexibility on conformations and functions of cohesin seem worthwhile.

The unusual phenotypes of *smc3-D667* are also strikingly similar to those described for Pds5p depletion and *mcd1* alleles (Chan *et al.*, 2013, Eng *et al.*, 2014). They all allow stable cohesin binding to DNA but cause defects in cohesion maintenance and condensation. The *smc3-D667* mutant reduces cohesin chromosome binding by 50%. Previous work demonstrated that reduction of cellular Mcd1p reduced cohesin binding to CARs by 50%, yet cohesion was established and maintained at nearly wild-type levels (Heidinger-Pauli *et al.*, 2010). This shows that merely reducing cohesin binding on chromosomes is not sufficient to produce a maintenance defect.

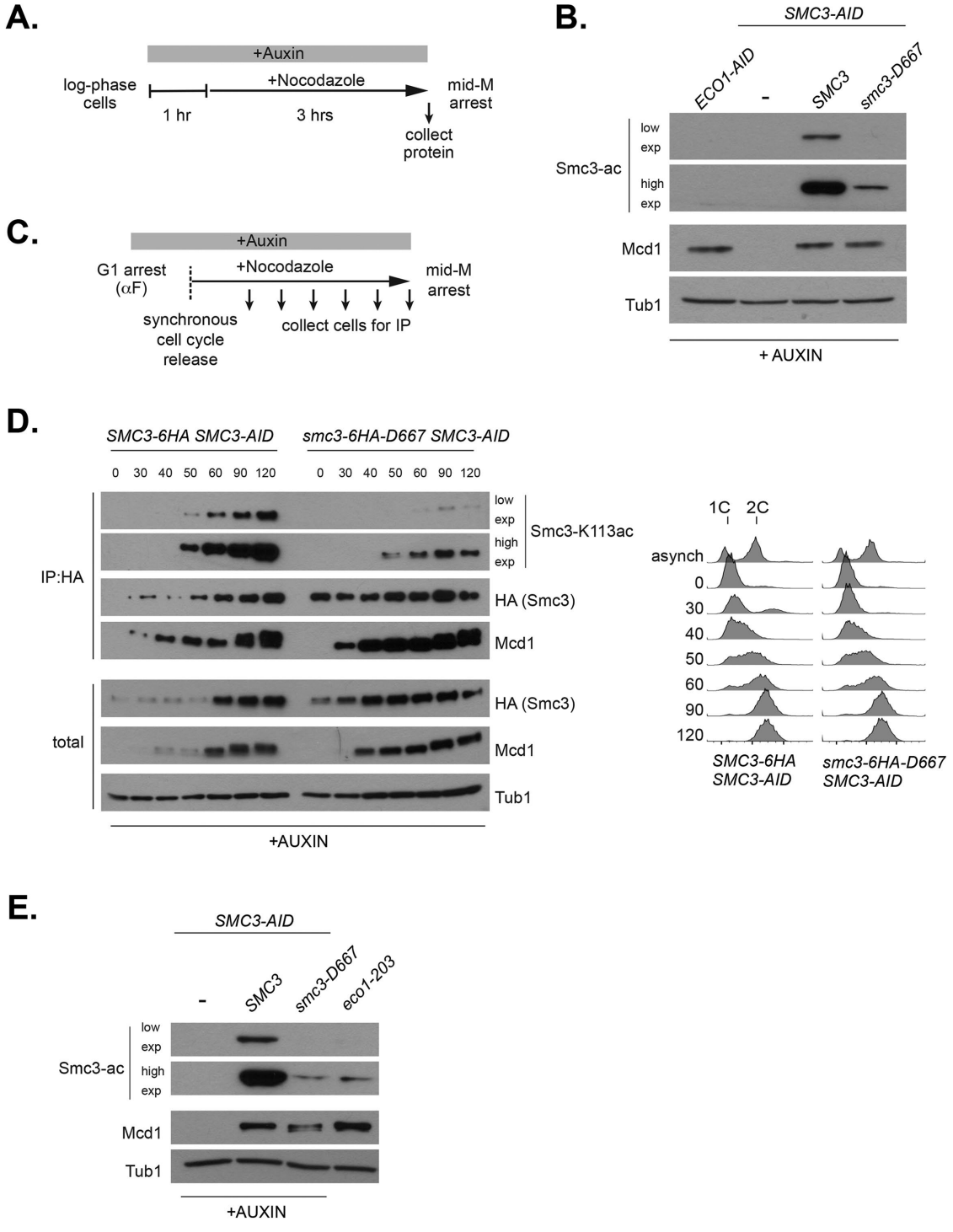

FIGURE 5: smc3-D667p has reduced acetylation at K113. (A) Regimen used to assess Smc3-K113 acetylation in mid–M phase–arrested cells. Early log phase cultures were treated with 0.75 mM auxin for 1 h to deplete Smc3-3V5-AIDp, and then nocodazole was added, and cultures were incubated 3 h to arrest cells in mid–M phase. (B) Reduced K113 acetylation of smc3-D667p. Haploid *ECO1-AID* (VG3633-2D), *SMC3-AID* (VG3651-3D), *SMC3 SMC3-AID* (BRY474), and *smc3-D667 SMC3-AID* (BRY482) cultures grown as described in A. Protein extracts were made and subjected to SDS–PAGE and then analyzed by Western blot. Antibodies against Smc3-K113 acetylation (Smc3-ac) are shown as short and long exposures; anti-Mcd1p antibodies (Mcd1p) serve as control for cohesin levels and antibodies against tubulin (Tub1) for a loading control. (C) Regimen used to determine the kinetics of Smc3-K113 acetylation establishment within a single cell cycle. Log phase cultures grown in YPD at 23°C were arrested in G1 using alpha factor, treated with auxin to deplete Smc3p-AID in G1, and then released into fresh YPD containing auxin and nocodazole to synchronously arrest cells in mid–M phase (*Materials and Methods*). (D) smc3-6HA-D667p has reduced acetylation in S phase but acetylation remains in mid–M phase. Haploid *SMC3-AID* cells expressing Smc3-6HAp (BRY604, left) or smc3-6HA-D667p (BRY602, right) were grown as described in C. Aliquots were taken at the indicated time points, and protein

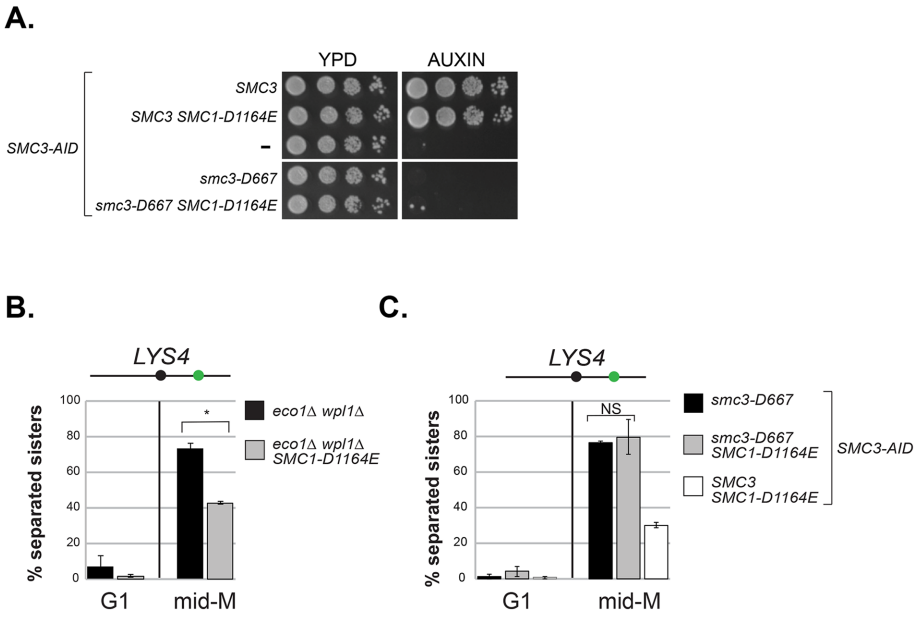

FIGURE 6: The *SMC1-D1164E* mutation fails to suppress the inviability or cohesion defect of *smc3-D667*. (A) *smc1-D1164E* failed to restore viability to *smc3-D667* cells. Haploid strains *SMC3 SMC3-AID* (BRY474), *SMC3 SMC3-AID SMC1-D1164E* (BRY832), *SMC3-AID* (VG3651-3D), *smc3-D667 SMC3-AID* (BRY482), and *smc3-D667 SMC3-AID SMC1-D1164E* (BRY833) were grown to saturation in YPD and then plated as 10-fold serial dilutions onto YPD alone (YPD) or containing 0.75 mM auxin (YPD + auxin) and incubated 2 d at 23°C. (B) *SMC1-D1164E* suppresses cohesion loss of the *eco1Δ wpl1Δ* mutant in mid–M phase–arrested cells. Haploid strains *eco1Δ wpl1Δ* (VG3503-4A) and *SMC1-D1164E eco1Δ wpl1Δ* (VG3575-2C) grown as described in Figure 2A. Cells from G1 and mid–M phase arrest were fixed and processed and scored for cohesion loss at the *CEN*-distal *LYS4* locus. *$p < 0.05$ (*t* test, two-tailed). (C) *SMC1-D1164E* fails to suppress cohesion loss of *smc3-D667* cells. Haploid strains *smc3-D667 SMC3-AID* (BRY482), *smc3-D667 SMC3-AID SMC1-D1164E* (BRY833), and *SMC3 SMC3-AID SMC1-D1164E* (BRY832) cells were grown according the regimen in Figure 2A and processed to assess cohesion loss at the *CEN*-distal *LYS4* locus as described in B. For both B and C, the percentage of cells with two GFP foci (sister separation) were derived from two independent experiments. An amount of 100–200 cells was scored per sample at each time point. Error bars represent SD. NS = not significant ($p = 0.74$; *t* test, two-tailed).

Therefore, the reduced chromosomal binding of cohesin in the *smc3-D667* mutant is unlikely to be the major cause of its maintenance defect. Rather, an additional activity of cohesin must be impaired (see below). Interestingly, the *mcd1-ROCC* mutant displays a cohesion maintenance defect yet cohesin binds at wild-type levels (Eng *et al.*, 2014). This result suggests that *smc3-D667*, *mcd1-ROCC*, and *pds5* mutants may render cohesin sensitive to a cohesion antagonizing pathway active late in the cell cycle, but our results suggest that at least for *smc3-D667*, this putative pathway would have to be independent of Wpl1p function or Smc3p-K112,K113 acetylation. Further investigation will be necessary to better understand the mechanistic underpinnings of cohesion maintenance.

Our observation that the Smc3p hinge also functions in cohesion maintenance suggests that it may cooperate alongside Pds5p and Mcd1p to promote a common molecular function. Indeed, this common function provides a biological explanation for in vivo FRET studies that suggest the formation of a complex involving the head, hinge, and Pds5p (Mc Intyre *et al.*, 2007), and recent biochemical experiments that detected a supramolecular complex between the *Schizosaccharomyces pombe* hinge dimer and Psc3p (Scc3p orthologue) that binds to the head-associated Rad21p (Mcd1p orthologue) and Pds5p. Altogether these biochemical results along with our study support the idea that the hinge, Mcd1p, and Pds5p cooperate in a structural conformation required to promote cohesion maintenance and condensation.

Potential insight into the molecular function of this complex conformation comes from several additional observations. One possibility was the protection of Eco1p acetylation of Smc3p. Here we show that while the level of smc3-D667 acetylation is lower than wild type, it is equal to that of the *eco1-203* mutant at its permissive temperature, which supports both viability and sister chromatid cohesion. Furthermore, we show that *SMC1-D1164E* and *wpl1Δ*, two different mutations previously shown to bypass the absence of Eco1p acetylation in viability, cohesion (only *smc1-D1164E*) and condensation (only *wpl1Δ*) are unable to restore these functions to the *smc3-D667* mutant. Finally, while Pds5p depletion also shows reduced Smc3p acetylation, the *mcd1-ROCC* allele does not (Chan *et al.*, 2013; Robison, unpublished data), again separating the function of this complex conformation in cohesion maintenance from additional functions it may have in promoting acetylation.

A second possibility stems from our observation that the D667 region of the hinge is necessary for the communication between cohesin complexes as revealed by interallelic complementation. We showed that *smc3-D667* was unable to complement the inviability of *smc3-42* in *trans*. We previously showed viability of *smc3-42* could be complemented by chromosome bound *smc3-K113R*. Furthermore, the interallelic complementation for viability reflected restoration of all cohesin's biological functions and restoration of

extracts were made. A small portion was reserved for total protein, and then anti-HA antibody was added to immunoprecipitate Smc3-6HAp or smc3-6HA-D667p (*Materials and Methods*). Samples were subjected to SDS–PAGE and then analyzed by Western blot. Antibodies against Smc3-K113 acetylation (Smc3-ac) and both short and long exposures are shown for better comparison. Antibodies were used to monitor levels of the Smc3p (HA) and Mcd1p (Mcd1) cohesin subunits and anti-Tubulin antibodies (Tub1) used as a loading control. Samples were also collected to assess DNA content by flow cytometry (right side). (E) Similar levels of K113 acetylation in *smc3-D667* and *eco1-203* at permissive temperature. Haploid strains *SMC3-AID* (VG3651-3D), *SMC3 SMC3-AID* (BRY474), *smc3-D667 SMC3-AID* (BRY482), and *eco1-203* (VG3506-5D) were treated as described in A. Protein extracts were made and then subjected to SDS–PAGE and Western blot analysis. Antibodies against Smc3-K113 acetylation (Smc3-ac) and both short and long exposures are shown for better comparison. Anti-MCD1 antibodies (Mcd1) were used as a control for cohesin levels and anti-Tubulin antibodies (Tub1) for a loading control.

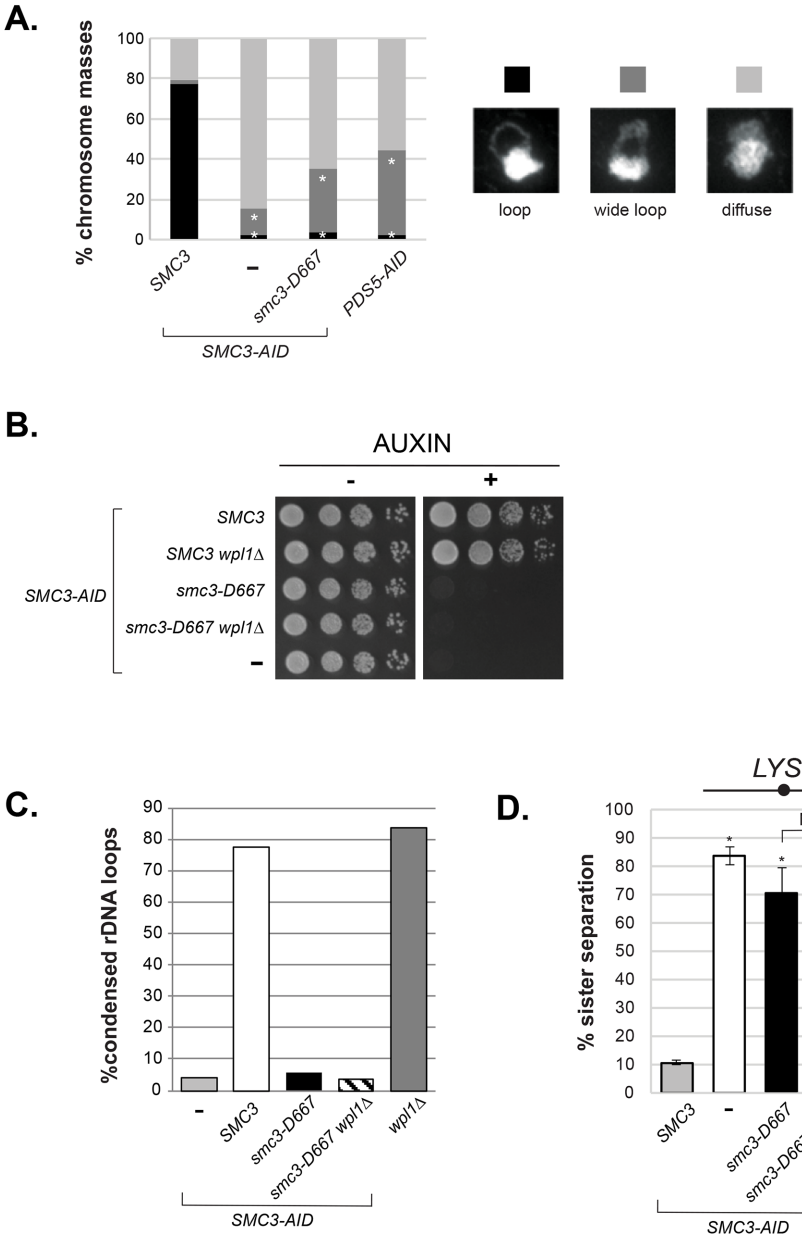

FIGURE 7: The *smc3-D667* mutant is defective in condensation and cohesion even in the absence of cohesin antagonist Wpl1p. (A) Condensation of the *rDNA* locus in *smc3-D667* cells. Percentage of chromosome masses displaying tight loop, wide loop, or diffuse *rDNA* morphologies. Haploid strains *SMC3 SMC3-AID* (BRY474), *SMC3-AID* (VG3651-3D), *smc3-D667 SMC3-AID* (BRY482), and *PDS5-AID* (TE228) were grown and treated as in Figure 2A and then processed as if for in situ hybridization (see *Materials and Methods*). Chromosome masses were scored for *rDNA* locus morphology after staining with DAPI. $n = 200$ for each genotype. *$p < 0.05$ (when compared with *SMC3 SMC3-AID* masses; chi-squared). Data were collected from two independent experiments. (B) *wpl1*Δ fails to restore viability to *smc3-D667* cells. Haploid *SMC3-AID* strain derivatives with *SMC3* (BRY474), *SMC3 wpl1*Δ (BRY716), *smc3-D667* (BRY482), *smc3-D667 wpl1*Δ (BRY718), or *SMC3-AID* alone (VG3651-3D) were grown and plated as described in Figure 1C. (C) Quantification of condensed *rDNA* masses from mid–M phase–arrested cells. Haploid strains *SMC3-AID* (VG3651-3D), *SMC3 SMC3-AID* (BRY474), *smc3-D667 SMC3-AID* (BRY482), *smc3-D667 SMC3-AID wpl1*Δ (BRY718), and *wpl1*Δ (DK5561) were treated and processed as in A. The percentage of chromosome masses displaying a tight *rDNA* loop is shown. (D) Cohesion loss in *smc3-D667 wpl1*Δ cells. Haploid *wpl1*Δ (DK5561) and *SMC3-AID* strain derivatives with *SMC3* (BRY474), *SMC3-AID* alone (VG3651-3D), *smc3-D667* (BRY482), and *smc3-D667 wpl1*Δ (BRY718) were treated as in Figure 2A, and the percentages of separated sisters at the *LYS4* locus were plotted. *$p < 0.05$ when tested against *SMC3 SMC3-AID* (*t* test, two-tailed). NS = not significant ($p = 0.25$). Error bars represent the SD.

smc3-42p binding to DNA (Eng *et al.*, 2015). Similar phenotypic and molecular interallelic complementation for *mcd1* alleles was also observed (Eng *et al.*, 2015). These observations led us to suggest that interallelic complementation of cohesin mutants reflected cohesin communication likely by the physical interaction between cohesin complexes. The importance of SMC complex oligomerization in their function is gaining traction. The inability of *smc3-D667* to complement *smc3-42* is consistent with the idea that the D667 region of the hinge is necessary for the physical interaction between cohesins, and this physical interaction is necessary for maintaining cohesion and condensation.

We propose a working model in which cohesin oligomerizes by forming inverted dimers such that the hinge of one cohesin binds to the head of the other cohesin possibly through binding to Scc3p and that this hinge-head interaction is stabilized by Pds5p. As suggested previously, we can imagine two ways in which hinge-dependent oligomerization might be critical for maintenance of tethering (Eng *et al.*, 2015). We previously showed that mere binding of cohesin to DNA is insufficient to generate tethering, implying that tethering requires an additional activity (Eng *et al.*, 2014). In one model (intramolecular handcuff), two DNA binding activities reside in the same cohesin. In this case, oligomerization may inhibit (possibly by physical occlusion) factors that destabilize one of these binding activities. In a second model (intermolecular handcuff) tethering is achieved directly by hinge-dependent oligomerization of two cohesins each of which has a single DNA binding activity. Resolving these models awaits direct biochemical assays for cohesin oligomerization.

MATERIALS AND METHODS

Random insertion screen of *SMC3*

Plasmid pBR25 containing *pGAL-SMC3 URA3 ARS/CEN* was subject to in vitro transposition according to the protocol recommended by the MuA transposase MGS Kit (ThermoFisher Cat. F701). After transforming into TOP10 cells (Thermo), 5756 AmpR KanR colonies were pooled, and plasmids were harvested by Midi Prep (Qiagen). The pooled library was digested with *Not*I to excise the KanR marker, gel extracted, and religated. Ligation products were transformed once again into TOP10 cells and confirmed to have lost KanR by replica plating. More than 30,000 colonies were pooled, and plasmids were harvested by Midi Prep to obtain a library of *pGAL-SMC3* plasmids with 15 extra

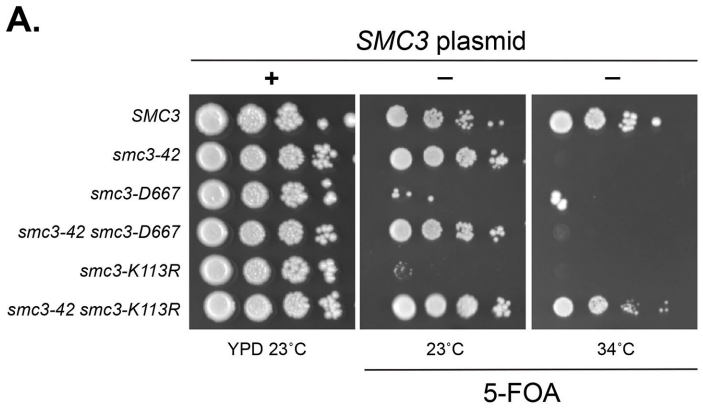

B.

Genotype	Viability 23˚C	Viability 34˚C	Interallelic complementation
smc3-42	+	–	N/A
smc3-K113R	–	–	N/A
smc3-D667	–	–	N/A
smc3-42 smc3-K113R	+	+	YES
smc3-42 smc3-D667	+	–	NO

FIGURE 8: The D667 region is necessary for interallelic complementation. (A) Assessing whether *smc3-D667* complements the *smc3-42* mutant. Haploid strains *SMC3* (VG3486), *smc3-42* (TE576), *smc3-D667* (BRY467), *smc3-42 smc3-D667* (BRY756), *smc3-K113R* (VG3486-K113R), and *smc3-42 smc3-K113R* (TE578) all contain the *SMC3 URA3 CEN* plasmid. Strains were grown to saturation in YPD cultures to allow loss of the *SMC3 URA3 CEN* plasmid and then played at 10-fold serial dilutions on YPD or FOA plates and incubated at the indicated temperatures. (B) Table summarizes interallelic complementation of haploid cells harboring the temperature-sensitive *smc3-42* allele (Eng *et al.*, 2015) and A.

nucleotides randomly inserted. Library depth was calculated by multiplying the fraction of pBR25 coding for *SMC3* (3,693 base pairs of 10,083 base pairs total) by the number of AmpR KanR colonies (5756) to obtain 2118 plasmids expected to have an insertion in *SMC3*. From this calculation, we expect plasmids represented in the library harboring insertions every ~1.7 base pairs along *SMC3*. The library was transformed into wild-type (3349-1B) and *smc3-42* (3358-3B) strains, which were incubated at 23°C for 3 d to select for transformants on synthetic complete media lacking uracil (SC –URA) with 2% dextrose supplied as the carbon source. Wild-type colonies (3382) and *smc-42* colonies (1811) were screened. Transformation colonies were replica plated onto SC –URA 2% galactose plates and SC –URA 2% dextrose plates as a control and incubated overnight at 23°C. Colonies that were slow growing or inviable on galactose plates were then grown overnight in liquid YPD and plated in 10-fold serial dilutions on 1) galactose plates to confirm slow growth and 2) 5-fluoroorotic acid (FOA) plates with 2% galactose to confirm linkage of slow growth to presence of the RID library plasmid. Insertion mutations were identified by PCR and sequencing across the entire *SMC3* open reading frame (ORF) .

Yeast strains, media, and growth

All strains used are in the A364A background, and their genotypes can be found in Table 1. Yeast extract/peptone/dextrose media and synthetic dropout media were prepared as previously described (Guacci *et al.*, 1997). Conditional AID degron strains were grown in YPD and auxin (3-indoleacetic acid; Sigma Aldrich Cat. I3750) added to a final concentration of 0.75 mM to deplete AID-tagged proteins. YPD agar plates supplemented with auxin were made by cooling molten YPD 2% agar to 55°C prior to addition of auxin.

Cohesion assays

Sister chromatid cohesion was assessed at either the centromere-distal *LYS4* locus or the centromere-proximal *TRP1* locus on chromosome IV in which *LacO* arrays had been integrated. The *GFP-LacI* fusion allele integrated at *HIS3* allows fluorescence microscopic visualization of *LacO* arrays. Cohesion was scored by growing cells to mid–log phase (OD600 ~0.3) and arresting them in G1 using alpha factor at 10^{-8} M (Sigma-Aldrich T6901-5MG). After arresting for 3 h, auxin was added to a final concentration of 0.75 mM to deplete Smc3-AIDp for 1 h. Cells were released from G1 arrest by washing in YPD containing auxin and 0.1 mg/ml Pronase E (Sigma Aldrich) five times and resuspending in YPD containing auxin and 15 µg/ml nocodozole (Sigma Aldrich). Cultures were incubated at 23°C and samples fixed either 1) periodically for assessing S-phase cohesion establishment or 2) after 3 h in which >95% of cells had arrested in G2/M. In addition to fixation for microscopy, samples were taken in parallel to assess DNA content by flow cytometry. Cohesion was scored by counting the GFP-LacI foci in the nucleus by fluorescence microscopy of fixed cells.

Monitoring condensation at the *rDNA* locus

Cells were grown as if for assessing cohesion by arresting in YPD containing auxin and nocodazole following release from G1. Cells were fixed, spheroplasted, and lysed to allow binding of chromosomes to slides as described previously (Guacci *et al.*, 1994). Briefly, 1 ml of mid–M phase–arrested cells were fixed 2 h in 100 µl of 37% formaldehyde, washed twice in water, and spheroplasted for 1 h. Triton X-100 was added to 0.5% for 5 min, and then cells were pelleted and resuspended in water. Cells were then added to poly-lysine–coated slides for 10 min. SDS (0.5%) was added for 10 min to solubilize membranes and release DNA masses and then removed. Slides were fixed in 3:1 methanol:acetic acid for 5 min and allowed

Strain	Genotype	Reference
BRY467	*MATa smc3-D667-LEU2:leu2-3,112 smc3Δ::HPH lys4::LacO(DK)-NAT bar1 pHIS3-GFPLacI-TRP1:his3-11,15 trp1-1 ura3-52* + pEU42 (*SMC3 CEN URA3*)	This study
BRY474	*MATa SMC3-LEU2:leu2-3,112 SMC3-3V5-AID^{608} trp1Δ::OsTIR1-CaTRP1 lys4::LacO(DK)-NAT pHIS3-GFPLacI-HIS3:his3-11,15 ura3-52 bar1*	This study
BRY482	*MATa smc3-D667-LEU2:leu2-3,112 SMC3-3V5-AID^{608} trp1Δ::OsTIR1-CaTRP1 lys4::LacO(DK)-NAT pHIS3-GFPLacI-HIS3:his3-11,15 ura3-52 bar1*	This study
BRY602	*MATa smc3-6HA^{608}-D667-URA3:ura3-52 SMC3-3V5-AID^{608} trp1Δ::OsTIR1-CaTRP1 lys4::LacO(DK)-NAT leu2-3,112 pHIS3-GFPLacI-HIS3:his3-11,15 bar1*	This study
BRY604	*MATa SMC3-6HA^{608}-URA3:ura3-52 SMC3-3V5-AID^{608} trp1Δ::OsTIR1-CaTRP1 lys4::LacO(DK)-NAT leu2-3,112 pHIS3-GFPLacI-HIS3:his3-11,15 bar1*	This study
BRY607	*MATa SCC3-3FLAG^{1089}-LEU2:leu2-3,112 SMC3-3V5-AID^{608} trp1Δ::OsTIR1-CaTRP1 lys4::LacO(DK)-NAT pHIS3-GFPLacI-HIS3:his3-11,15 leu2-3,112 ura3-52 bar1*	This study
BRY621	*MATa SCC3-3FLAG^{1089}-LEU2:leu2-3,112 SMC3-6HA^{608}-URA3:ura3-52 SMC3-3V5-AID^{608} trp1Δ::OsTIR1-CaTRP1 lys4::LacO(DK)-NAT pHIS3-GFPLacI-HIS3:his3-11,15 bar1*	This study
BRY625	*MATa SCC3-3FLAG^{1089}-LEU2:leu2-3,112 smc3-6HA^{608}-D667-URA3:ura3-52 SMC3-3V5-AID^{608} trp1Δ::OsTIR1-CaTRP1 lys4::LacO(DK)-NAT pHIS3-GFPLacI-HIS3:his3-11,15 bar1*	This study
BRY647	*MATa SMC3-LEU2:leu2-3,112 smc3Δ::HPH rad61Δ::G418 lys4::LacO(DK)-NAT ura3-52 bar1 pHIS3-GFPLacI-TRP1:his3-11,15 trp1-1* + pEU42 (*SMC3 CEN URA3*)	This study
BRY648	*MATa SMC3(D1189H)-LEU2:leu2-3,112 smc3Δ::HPH rad61Δ::G418 lys4::LacO(DK)-NAT ura3-52 bar1 pHIS3-GFPLacI-TRP1:his3-11,15 trp1-1* + pEU42 (*SMC3 CEN URA3*)	Guacci *et al.* (2015)
BRY649	*MATa smc3-D667-LEU2:leu2-3,112 smc3Δ::HPH rad61Δ::G418 lys4::LacO(DK)-NAT ura3-52 bar1 pHIS3-GFPLacI-TRP1:his3-11,15 trp1-1* + pEU42 (*SMC3 CEN URA3*)	This study
BRY650	*MATa smc3-D667-D1189H-LEU2:leu2-3,112 smc3Δ::HPH rad61Δ::G418 lys4::LacO(DK)-NAT ura3-52 bar1 pHIS3-GFPLacI-TRP1:his3-11,15 trp1-1* + pEU42 (*SMC3 CEN URA3*)	This study
BRY676	*MATa SMC3-3V5-AID^{608} trp1Δ::OsTIR1-CaTRP1 LacO(DK)-NAT:10kb-CEN4 pHIS3-GFPLacI-HIS3:his3-11,15 ura3-52 leu2-3,112 bar1*	This study
BRY678	*MATa SMC3-LEU2:leu2-3,112 SMC3-3V5-AID^{608} trp1Δ::OsTIR1-CaTRP1 LacO(DK)-NAT:10kb-CEN4 pHIS3-GFPLacI-HIS3:his3-11,15 ura3-52 bar1*	This study
BRY680	*MATa smc3-D667-LEU2:leu2-3,112 SMC3-3V5-AID^{608} trp1Δ::OsTIR1-CaTRP1 LacO(DK)-NAT:10kb-CEN4 pHIS3-GFPLacI-HIS3:his3-11,15 ura3-52 bar1*	This study
BRY714	*MATa rad61Δ::HPHMX SMC3-3V5-AID^{608} trp1Δ::OsTIR1-CaTRP1 lys4::LacO(DK)-NAT leu2-3,112 pHIS3-GFPLacI-HIS3:his3-11,15 ura3-52 bar1*	This study
BRY716	*MATa rad61Δ::HPHMX SMC3-LEU2:leu2-3,112 SMC3-3V5-AID^{608} trp1Δ::OsTIR1-CaTRP1 lys4::LacO(DK)-NAT pHIS3-GFPLacI-HIS3:his3-11,15 ura3-52 bar1*	This study
BRY718	*MATa rad61Δ::HPHMX smc3-D667-LEU2:leu2-3,112 SMC3-3V5-AID^{608} trp1Δ::OsTIR1-CaTRP1 lys4::LacO(DK)-NAT pHIS3-GFPLacI-HIS3:his3-11,15 ura3-52 bar1*	This study
BRY720	*MATa smc1-D1164E SMC3-3V5-AID^{608} trp1Δ::OsTIR1-CaTRP1 lys4::LacO(DK)-NAT leu2-3,112 pHIS3-GFPLacI-HIS3:his3-11,15 ura3-52 bar1*	This study
BRY721	*MATa CDC20-3V5-AID2-KANMX smc3-D667-LEU2:leu2-3,112 SMC3-3V5-AID^{608} trp1Δ::OsTIR1-CaTRP1 lys4::LacO(DK)-NAT pHIS3-GFPLacI-HIS3:his3-11,15 ura3-52 bar1*	This study
BRY723	MATa *CDC20-3V5-AID2-KANMX SMC3-3V5-AID^{608} trp1Δ::OsTIR1-CaTRP1 lys4::LacO(DK)-NAT leu2-3,112 pHIS3-GFPLacI-HIS3:his3-11,15 ura3-52 bar1*	This study
BRY724	MATa *CDC20-3V5-AID2-KANMX SMC3-LEU2:leu2-3,112 SMC3-3V5-AID^{608} trp1Δ::OsTIR1-CaTRP1 lys4::LacO(DK)-NAT pHIS3-GFPLacI-HIS3:his3-11,15 ura3-52 bar1*	This study
BRY756	*MATa smc3-D667-LEU2:leu2-3,112 smc3-42 lys4::LacO(DK)-NAT trp1-1 pHIS3-GFPLacI-HIS3:his3-11,15 bar1 ura3-52* + pEU42 (*SMC3 CEN URA3*)	This study
BRY815	*MATa PDS5-3V5-AID2:KanMx6 LacO(DK)-NAT:10kb-CEN4 pHIS3-GFP-LacI-HIS3::his3-11,15 trp1-1 leu2-3,112 bar1 GAL+ ADH1-OsTIR1-URA3::ura3-52*	This study

TABLE 1: Strains.

Continues

Strain	Genotype	Reference
BRY832	*MATa smc1-D1164E SMC3-LEU2::leu2-3,112 SMC3-3V5-AID^{608} trp1Δ::OsTIR1-CaTRP1 lys4::LacO(DK)-NAT pHIS3-GFPLacI-HIS3:his3-11,15 ura3-52 bar1*	This study
BRY833	*MATa SMC1-D1164E smc3-D667-LEU2::leu2-3,112 SMC3-3V5-AID^{608} trp1Δ::OsTIR1-CaTRP1 lys4::LacO(DK)-NAT pHIS3-GFPLacI-HIS3:his3-11,15 ura3-52 bar1*	This study
BRY840	*MATa SCC2-3FLAG-AID2-HPHMX SMC3-N607-6HA-URA3:ura3-52 SMC3-3V5-AID^{608} trp1Δ::OsTIR1-CaTRP1 lys4::LacO(DK)-NAT leu2-3,112 pHIS3-GFPLacI-HIS3:his3-11,15 bar1*	This study
BRY842	*MATa SCC2-3FLAG-AID2-HPHMX smc3-6HA^{608}-D667-URA3:ura3-52 SMC3-3V5-AID^{608} trp1Δ::OsTIR1-CaTRP1 lys4::LacO(DK)-NAT leu2-3,112 pHIS3-GFPLacI-HIS3:his3-11,15 bar1*	This study
BRY865	*MATa smc3-D667A-LEU2:leu2-3,112 SMC3-3V5-AID^{608} trp1Δ::pGPD1-TIR1-CaTRP1 lys4::LacO(DK)-NAT pHIS3-GFPLacI-HIS3:his3-11,15 ura3-52 bar1*	This study
BRY866	*MATa smc3-D667A,K668A,R669A-LEU2:leu2-3,112 SMC3-3V5-AID^{608} trp1Δ::pGPD1-TIR1-CaTRP1 lys4::LacO(DK)-NAT pHIS3-GFPLacI-HIS3:his3-11,15 ura3-52 bar1*	This study
DK5535	*MATa mcd1-Q266-3FLAG-URA3::ura3-52 MCD1-AID-KANMX pGPD1-OsTIR1-LEU2::leu2-3,112 lys4::LacO(DK)-NAT trp1-1 GFPLacI-HIS3:his3-11,15 bar1*	Eng *et al.* (2014)
DK5542	*MATa MCD1-AID-KANMX6 ADH1-OsTIR1-URA3::ura3-52 lys4::LacO(DK)-NAT trp1-1 GFPLacI-HIS3:his3-11,15 bar1 leu2-3,112*	Eng *et al.* (2014)
DK5561	*MATa rad61Δ::HPHMX pADH1-TIR1-URA3::ura3-42 lys4::LacO(DK)-NAT trp1-1 GFPLacI-HIS3:his3-11,15 bar1 leu2-3,112*	Eng *et al.* (2014)
TE228	*MATa PDS5-3V5-AID2-KANMX6 lys4::LacO(DK)-NAT pHIS3-GFP-LacI-HIS3::his3-11,15 trp1-1 ura3-52*	Eng *et al.* (2014)
TE576	*MATa smc3-42 lys4::LacO(DK)-NAT pHIS3-GFP-LacI-HIS3:his3-11,15 leu2-3,112 bar1 trp1-1* + pEU42 (*SMC3 CEN URA3*)	Eng *et al.* (2015)
TE578	*MATa smc3-42 smc3-K113R-LEU2::leu2-3,112 lys4::LacO(DK)-NAT pHIS3-GFP-LacI-HIS3:his3-11,15 leu2-3,112 bar1 trp1-1* + pEU42 (*SMC3 CEN URA3*)	Eng *et al.* (2015)
VG3349-1B	*MATa lys4::LacO(DK)-NAT trp1-1 GFPLacI-HIS3:his3-11,15 bar1 leu2-3,112 ura3-52*	Guacci and Koshland (2012)
VG3358-3B	*MATa smc3-42 lys4::LacO(DK)-NAT trp1-1 pHIS3-GFP-LACI-HIS3:his3-11,15 bar1 leu2-3,112 ura3-52*	Guacci and Koshland (2012)
VG3464-16C	*MATa smc3Δ::HPH lys4::LacO(DK)-NAT bar1 pHIS3-GFPLacI-TRP1:his3-11,15 trp1-1 leu2-3,112 ura3-52* +pEU42 (*SMC3 CEN URA3*)	Guacci and Koshland (2012)
VG3486	*MATa smc3Δ::HPH lys4::LacO(DK)-NAT bar1 pHIS3-GFPLacI-TRP1:his3-11,15 trp1-1 leu2-3,112 ura3-52* + pEU42 (*SMC3 CEN URA3*) + pEU41 (*SMC3 CEN LEU2*)	Eng *et al.* (2015)
VG3486-K113R	*MATa smc3Δ::HPH lys4::LacO(DK)-NAT bar1 pHIS3-GFPLacI-TRP1:his3-11,15 trp1-1 leu2-3,112 ura3-52* + pEU42 (*SMC3 URA3 CEN*) + *pEU41-K113R* (*smc3-K113R LEU2 CEN*)	Eng *et al.* (2015)
VG3503-4A	*MATa rad61Δ::HPHMX eco1Δ::KANMX trp1-1 lys4::LacO(DK)-NAT leu2-3,112 pHIS3-GFPLacI-HIS3:his3-11,15 ura3-52 bar1*	Çamdere *et al.* (2015)
VG3506-5D	*MATa eco1-203 LacO-NAT:10kb-CEN4 trp1-1 pHIS3-GFPLacI-HIS3:his3-11,15 leu2-3,112 ura3-52 bar1*	This study
VG3575-2C	*MATa smc1-D1164E rad61Δ::HPHMX eco1Δ::G418 lys4::LacO(DK)-NAT GFPLacI-HIS3:his3-11,15 trp1-1 leu2-3,112 ura3-52 bar1*	Çamdere *et al.* (2015)
VG3578-1A	*MATa smc3Δ::HPHMX rad61Δ::KANMX leu2-3,112 lys4::LacO(DK)-NAT ura3-52 bar1 pHIS3-GFPLacI-TRP1:his3-11,15 trp1-1* + pEU42 (*SMC3 CEN URA3*)	Guacci *et al.* (2015)
VG3620-4C	*MATa trp1Δ::pGPD1-TIR1-CaTRP1 lys4::LacO(DK)-NAT leu2-3,112 pHIS3-GFPLacI-HIS3:his3-11,15 ura3-52 bar1*	Çamdere *et al.* (2015)
VG3633-2D	*MATa ECO1-3V5-AID2-KANMX trp1Δ::pGPD1-TIR1-CaTRP1 lys4::LacO(DK)-NAT leu2-3,112 pHIS3-GFPLacI-HIS3:his3-11,15 bar1 ura3-52*	This study
VG3651-3D	*MATa SMC3-3V5-AID^{608} trp1Δ::pGPD1-TIR1-CaTRP1 lys4::LacO(DK)-NAT pHIS3-GFPLacI-HIS3:his3-11,15 leu2-3,112 ura3-52 bar1*	Çamdere *et al.* (2015)

TABLE 1: Strains. Continued

to dry. Cells on slides were treated with RNase A and Proteinase K and subject to a series of short 70, 80, 90, and 100% ethanol washes. After drying, DNA masses were visualized with 4′,6-diamidino-2-phenylindole (DAPI) and *rDNA* morphology scored.

Chromatin immunoprecipitation

Cells were grown as if for assessing cohesion by arresting at mid–M phase in yeast extract, peptone, and dextrose (YPD) containing auxin and nocodazole following release from G1 arrest. ChIP was performed as described previously (Wahba *et al.*, 2013; Eng *et al.*, 2014), except that chromatin shearing was performed on a Bioruptor Pico machine (Diagenode, Denville, NJ) for 5 min (30 s on/off cycling). Immunoprecipitation was performed using monoclonal mouse anti-HA (Roche), monoclonal mouse anti-V5 (ThermoFisher), polyclonal rabbit anti-Pds5p (Covance Biosciences, Princeton, NJ), or polyclonal rabbit anti-Mcd1p (Covance) antibodies. A no antibody control was always included to assess specificity of chromatin recovery.

Detection of Smc3-K113 acetylation by Western blotting

Cells were grown to OD_{600} = 0.5 in YPD at 23°C before addition of auxin to 0.75 mM and incubation for 1 h. Nocodazole was added to a final concentration of 15 µg/ml to arrest cells in mid–M phase. Cells were pelleted and resuspended in lysis buffer consisting of 25 mM HEPES, pH 8.0, 2 mM $MgCl_2$, 100 µM EDTA, 500 µM egtazic acid (EGTA), 1% NP-40, 150 mM KCl, 15% glycerol, Complete-Mini EDTA-free protease inhibitor cocktail (Roche), 10 mM sodium butyrate, and 20 mM beta-glycerophosphate. Cells were incubated in buffer for 30 min on ice, and then glass beads were added to a 1:1 volume ratio before bead beating for 3 min. Lysates were pelleted at 14,000 rpm for 10 min at 4°C, and protein concentration was measured using Coomassie Brilliant Blue. Lysates were boiled in 120 mM HEPES, pH 7.0, containing 1% SDS at 95°C for 5 min and then diluted 1:1 in 2× Laemmli sample buffer. Smc3-K113 acetylation was detected by blotting with monoclonal mouse antibody (a gift from K. Shirahige, University of Tokyo) at a concentration of 1:1000 in 5% milk-PBST.

Chromosome spreads and microscopy

Cells were grown as if for assessing cohesion by arresting in mid–M phase in YPD containing auxin and nocodazole following release from G1 arrest. Chromosome spreads were prepared as described previously (Wahba *et al.*, 2013). Slides were incubated with 1:5000 rabbit polyclonal anti-Mcd1p and 1:5000 mouse anti-V5 antibody (Life Technologies). Antibodies were diluted in blocking buffer (5% BSA, 0.2% milk, 1× phosphate-buffered saline, 0.2% Triton X-100). Secondary Alexa Fluor 488–congugated chicken anti-mouse and Alexa Fluor 568–congugated donkey anti-rabbit (ThermoFisher Cats. A21200 and A10042) antibodies were diluted 1:5000 in blocking buffer. Indirect immunofluorescence was detected on an Axioplan2 microscope (Zeiss, Thornwood, NY) using the 100× objective (numerical aperture 1.40) which is equipped with a Quantix charge-coupled camera (Photometrics).

ACKNOWLEDGMENTS

We thank Thomas Eng for helpful experimental guidance and Michelle Bloom, Rebecca Lamothe, Hugo Tapia, Gamze Çamdere, Lorenzo Costantino, Kristian Carlborg, Siheng Xiang, and Jeremiah Stricklin for fruitful discussions and reagents. The yeast Smc3-K113 acetylation antibody was a kind gift of Katsuhiko Shirahige. We also thank Benjamin Rowland and Ahmed Elbatsh for advice using the Smc3-K113 acetylation antibody. This work was funded by the National Institutes of Health (GM118189).

REFERENCES

Beckouët F, Hu B, Roig MB, Sutani T, Komata M, Uluocak P, Katis VL, Shirahige K, Nasmyth K (2010). An Smc3p acetylation cycle is essential for establishment of sister chromatid cohesion. Mol Cell 39, 689–699.

Çamdere G, Guacci V, Stricklin J, Koshland D (2015). The ATPases of cohesin interface with regulators to modulate cohesin-mediated DNA tethering. eLife 4, 13115.

Chan K-L, Gligoris T, Upcher W, Kato Y, Shirahige K, Nasmyth K, Beckouët F (2013). Pds5p promotes and protects cohesin acetylation. Proc Natl Acad Sci USA 110, 13020–13025.

Ciosk R, Shirayama M, Shevchenko A, Tanaka T, Tóth A, Shevchenko A, Nasmyth K (2000). Cohesin's binding to chromosomes depends on a separate complex consisting of Scc3p and Scc4p proteins. Mol Cell 5, 243–254.

D'Ambrosio LM, Lavoie BD (2014). Pds5p prevents the PolySUMO-dependent separation of sister chromatids. Curr Biol 24, 361–371.

Duncan FE, Hornick JE, Lampson MA, Schultz RM, Shea LD, Woodruff TK (2012). Chromosome cohesion decreases in human eggs with advanced maternal age. Aging Cell 11, 1121–1124.

Elbatsh AMO, Haarhuis JHI, Petela N, Chapard C, Fish A, Celie PH, Stadnik M, Ristic D, Wyman C, Medema R, *et al.* (2016). Cohesin releases DNA through asymmetric ATPase-driven ring opening. Mol Cell 61, 575–588.

Eng T, Guacci V, Koshland D (2014). ROCC, a conserved region in cohesin's Mcd1p subunit, is essential for the proper regulation of the maintenance of cohesion and establishment of condensation. Mol Biol Cell 25, 2351–2364.

Eng T, Guacci V, Koshland D (2015). Interallelic complementation provides functional evidence for cohesin-cohesin interactions on DNA. Mol Biol Cell 26, 4224–4235.

Glynn EF, Megee PC, Yu H-G, Mistrot C, Unal E, Koshland DE, DeRisi JL, Gerton JL (2004). Genome-wide mapping of the cohesin complex in the yeast Saccharomyces cerevisiae. PLoS Biol 2, E259.

Gruber S, Arumugam P, Katou Y, Kuglitsch D, Helmhart W, Shirahige K, Nasmyth K (2006). Evidence that loading of cohesin onto chromosomes involves opening of its SMC hinge. Cell 127, 523–537.

Guacci V, Hogan E, Koshland D (1994). Chromosome condensation and sister chromatid pairing in budding yeast. J Cell Biol 125, 517–530.

Guacci V, Koshland D (2012). Cohesin-independent segregation of sister chromatids in budding yeast. Mol Biol Cell 23, 729–739.

Guacci V, Koshland D, Strunnikov A (1997). A direct link between sister chromatid cohesion and chromosome condensation revealed through the analysis of MCD1 in S. cerevisiae. Cell 91, 47–57.

Guacci V, Stricklin J, Bloom MS, Guō X, Bhatter M, Koshland D (2015). A novel mechanism for the establishment of sister chromatid cohesion by the ECO1 acetyltransferase. Mol Biol Cell 26, 117–133.

Haering CH, Löwe J, Hochwagen A, Nasmyth K (2002). Molecular architecture of SMC proteins and the yeast cohesin complex. Mol Cell 9, 773–788.

Hartman T, Stead K, Koshland D, Guacci V (2000). Pds5p Is an essential chromosomal protein required for both sister chromatid cohesion and condensation in Saccharomyces cerevisiae. J Cell Biol 151, 613–626.

Heidinger-Pauli JM, Mert O, Davenport C, Guacci V, Koshland D (2010). Systematic reduction of cohesin differentially affects chromosome segregation, condensation, and DNA repair. Curr Biol 20, 957–963.

Heidinger-Pauli JM, Unal E, Koshland D (2009). Distinct targets of the Eco1 acetyltransferase modulate cohesion in S Phase and in response to DNA damage. Mol Cell 34, 311–321.

Hirano M, Anderson DE, Erickson HP, Hirano T (2001). Bimodal activation of SMC ATPase by intra- and inter-molecular interactions. EMBO J 20, 3238–3250.

Hons MT, Veld PJHIT, Kaesler J, Rombaut P, Schleiffer A, Herzog F, Stark H, Peters JM (2016). Topology and structure of an engineered human cohesin complex bound to Pds5B. Nat Commun 7, 12523.

Huis in t Veld PJ, Herzog F, Ladurner R, Davidson IF, Piric S, Kreidl E, Bhaskara V, Aebersold R, Peters JM (2014). Characterization of a DNA exit gate in the human cohesin ring. Science 346, 968–972.

Kamada K, Su'etsugu M, Takada H, Miyata M, Hirano T (2017). Overall shapes of the SMC-ScpAB complex are determined by balance between constraint and relaxation of its structural parts. Structure 25, 603–616 e4.

Kulemzina I, Ang K, Zhao X, Teh J-T, Verma V, Suranthran S, Chavda AP, Huber RG, Eisenhaber B, Eisenhaber F, *et al.* (2016). A reversible association between Smc coiled coils is regulated by lysine acetylation and is rrequired for cohesin association with the DNA. Mol Cell 63, 1044–1054.

Kurze A, Michie KA, Dixon SE, Mishra A, Itoh T, Khalid S, Strmecki L, Shirahige K, Haering CH, Lowe J, *et al*. (2011). A positively charged channel within the Smc1/Smc3p hinge required for sister chromatid cohesion. EMBO J 30, 364–378.
Laloraya S, Guacci V, Koshland D (2000). Chromosomal addresses of the cohesin component Mcd1p. J Cell Biol 151, 1047–1056.
Lee B-G, Roig MB, Jansma M, Petela N, Metson J, Nasmyth K, Löwe J (2016). Crystal structure of the cohesin gatekeeper Pds5 and in complex with Kleisin Scc1. Cell Rep 14, 2108–2115.
Lengronne A, McIntyre J, Katou Y, Kanoh Y, Hopfner K-P, Shirahige K, Uhlmann F (2006). Establishment of sister chromatid cohesion at the S. cerevisiae replication fork. Mol Cell 23, 787–799.
Mc Intyre JM, Muller EG, Weitzer S, Snydsman BE, Davis TN, Uhlmann F (2007). In vivo analysis of cohesin architecture using FRET in the budding yeast Saccharomyces cerevisiae. EMBO J 26, 3783–3793.
Megee PC, Mistrot C, Guacci V, Koshland D (1999). The centromeric sister chromatid cohesion site directs Mcd1p binding to adjacent sequences. Mol Cell 4, 445–450.
Michaelis C, Ciosk R, Nasmyth K (1997). Cohesins: chromosomal proteins that prevent premature separation of sister chromatids. Cell 91, 35–45.
Milutinovich M, Ünal E, Ward C, Skibbens RV, Koshland D (2007). A multistep pathway for the establishment of sister chromatid cohesion. PLoS Genet 3, e12.
Mishra A, Hu B, Kurze A, Beckouët F, Farcas A-M, Dixon SE, Katou Y, Khalid S, Shirahige K, Nasmyth K (2010). Both interaction surfaces within cohesin's hinge domain are essential for its stable chromosomal association. Curr Biol 20, 279–289.
Muir KW, Kschonsak M, Li Y, Metz J, Haering CH, Panne D (2016). Structure of the Pds5-Scc1 complex and implications for cohesin function. Cell Rep 14, 2116–2126.
Murayama Y, Uhlmann F (2015). DNA entry into and exit out of the cohesin ring by an interlocking gate mechanism. Cell 163, 1628–1640.
Nishimura K, Fukagawa T, Takisawa H, Kakimoto T, Kanemaki M (2009). An auxin-based degron system for the rapid depletion of proteins in nonplant cells. Nat Methods 6, 917–922.
Noble D, Kenna MA, Dix M, Skibbens RV, Ünal E, Guacci V (2006). Intersection between the regulators of sister chromatid cohesion establishment and maintenance in budding yeast indicates a multi-step mechanism. Cell Cycle 5, 2528–2536.
Onn I, Heidinger-Pauli JM, Guacci V, Unal E, Koshland DE (2008). Sister chromatid cohesion: a simple concept with a complex reality. Annu Rev Cell Dev Biol 24, 105–129.
Orgil O, Matityahu A, Eng T, Guacci V, Koshland D, Onn I (2015). A conserved domain in the scc3 subunit of cohesin mediates the interaction with both mcd1 and the cohesin loader complex. PLoS Genet 11, e1005036.
Ouyang Z, Zheng G, Tomchick DR, Luo X, Yu H (2016). Structural basis and IP6 requirement for Pds5-dependent cohesin dynamics. Mol Cell 62, 248–259.
Panizza S, Tanaka T, Hochwagen A, Eisenhaber F, Nasmyth K (2000). Pds5 cooperates with cohesin in maintaining sister chromatid cohesion. Curr Biol 10, 1557–1564.
Rolef Ben-Shahar T, Heeger S, Lehane C, East P, Flynn H, Skehel M, Uhlmann F (2008). Eco1-dependent cohesin acetylation during establishment of sister chromatid cohesion. Science 321, 563–566.
Rowland BD, Roig MB, Nishino T, Kurze A, Uluocak P, Mishra A, Beckouet F, Underwood P, Metson J, Imre R, *et al*. (2009). Building sister chromatid cohesion: Smc3 acetylation counteracts an antiestablishment activity. Mol Cell 33, 763–774.
Sakai A, Hizume K, Sutani T, Takeyasu K, Yanagida M (2003). Condensin but not cohesin SMC heterodimer induces DNA reannealing through protein–protein assembly. EMBO J 22, 2764–2775.
Skibbens RV, Corson LB, Koshland D, Hieter P (1999). Ctf7p is essential for sister chromatid cohesion and links mitotic chromosome structure to the DNA replication machinery. Genes Dev 13, 307–319.
Stead K, Aguilar C, Hartman T, Drexel M, Meluh P, Guacci V (2003). Pds5p regulates the maintenance of sister chromatid cohesion and is sumoylated to promote the dissolution of cohesion. J Cell Biol 163, 729–741.
Tanaka K, Hao Z, Kai M, Okayama H (2001). Establishment and maintenance of sister chromatid cohesion in fission yeast by a unique mechanism. EMBO J 20, 5779–5790.
Tóth A, Ciosk R, Uhlmann F, Galova M, Schleiffer A, Nasmyth K (1999). Yeast cohesin complex requires a conserved protein, Eco1p(Ctf7), to establish cohesion between sister chromatids during DNA replication. Genes Dev 13, 320–333.
Ünal E, Heidinger-Pauli JM, Kim W, Guacci V, Onn I, Gygi SP, Koshland DE (2008). A molecular determinant for the establishment of sister chromatid cohesion. Science 321, 566–569.
Wahba L, Gore SK, Koshland D, Proudfoot N (2013). The homologous recombination machinery modulates the formation of RNA–DNA hybrids and associated chromosome instability. eLife 2, e00505.
Zhang J, Shi X, Li Y, Kim B-J, Jia J, Huang Z, Yang T, Xiaoyong F, Jung SY, Wang Y, *et al*. (2008). Acetylation of Smc3p by Eco1p is required for S phase sister chromatid cohesion in both human and yeast. Mol Cell 31, 1143–1151.